The Meteoritical Society

Meteoritics & Planetary Science 57, Nr 9, 1665–1687 (2022)
doi: 10.1111/maps.13893

Compositional and spectroscopic investigation of three ungrouped carbonaceous chondrites

Mehmet YESILTAS[1]*, Yoko KEBUKAWA[2], Timothy D. GLOTCH[3], Michael ZOLENSKY[4], Marc FRIES[4], Namik AYSAL[5], and Fatma S. TUKEL[5]

[1]Faculty of Aeronautics and Space Sciences, Kirklareli University, Kirklareli 39100, Turkey
[2]Faculty of Engineering, Yokohama National University, 240-8501 Yokohama, Japan
[3]Department of Geosciences, Stony Brook University, Stony Brook, New York 11790, USA
[4]Astromaterials Research and Exploration Science, Johnson Space Center, NASA, Houston, Texas 77058, USA
[5]Department of Geological Engineering, Istanbul University-Cerrahpasa, Istanbul 34320, Turkey
*Corresponding author. E-mail: myesiltas@knights.ucf.edu

(Received 05 January 2022; revision accepted 15 June 2022)

Abstract–Ungrouped carbonaceous chondrites are not easily classified into one of the well-established groups due to compositional/petrological differences and geochemical anomalies. Type 2 ungrouped carbonaceous chondrites represent a very small fraction of all carbonaceous chondrites. They can potentially represent different aspects of asteroids and their regolith material. By conducting a multitechnique investigation, we show that Queen Alexandra Range (QUE) 99038 and Elephant Moraine (EET) 83226 do not resemble type 2 carbonaceous chondrites. QUE 99038 exhibits coarse-grained matrix, Fe-rich rims on olivines, and an apparent lack of tochilinite, suggesting that QUE 99038 has been metamorphosed. Its polyaromatic organic matter structures closely resemble oxidized CV3 chondrites. EET 83226 exhibits a clastic texture with high porosity and shows similarities to CO3 chondrites. It consists of numerous large chondrules with fine-grained rims that are often fragmented and discontinuous and set within matrix, suggesting a formation mechanism for the rims in a regolith environment. The kind of processes that can result in such chemical compositions as in QUE 99038 and EET 83226 is currently not fully known and clearly presents a conundrum. Tarda is a highly friable carbonaceous chondrite with close resemblance to Tagish Lake (ungrouped C2 chondrite). It comprises different types of chondrules (some with Fe-rich rims), framboid magnetite, sulfides, carbonates, and phyllosilicate- and carbon-rich matrix, and is consistent with being an ungrouped C2 chondrite.

INTRODUCTION

Carbonaceous chondrites are among the most primitive samples of our solar system. They retain records of their origin, formation mechanisms, evolution, and secondary processes they underwent. This makes them excellent samples for studies to better understand asteroidal parent body processes and shed light on the early history of the solar system. Carbonaceous chondrites constitute ~4% of all known meteorites and are divided into nine subgroups (CI, CM, CO, CV, CK, CR, CH, CB, and CY) based on their molecular, chemical, and isotopic composition (King et al., 2019; Sears & Dodd, 1988; Weisberg et al., 2006). The CI, CM, and CR chondrites occur as petrological types 1–3 and are characterized by unequilibrated compositions with low temperature aqueous alteration products (Brearley, 2006; Zolensky et al., 1993). The CO, CV, and CK groups exhibit a range of compositions (from unequilibrated CO3.0 chondrites to equilibrated CK6 chondrites) and are the thermally metamorphosed groups; they experienced minimal, if any, aqueous alteration (Huss et al., 2006). The CH and CB groups are rather metal-rich (20–80 vol%) hydrated samples (Greshake et al., 2002; Weisberg et al., 2006). The CY group, which was only recently recognized, consists of meteorites that have distinct chemical and isotopic compositions, and members of this group suggest parent body aqueous alteration followed by severe thermal metamorphism (>500 °C; King et al., 2019). The CY group differs from most of the carbonaceous chondrite groups and presents close affinity to CI chondrites (King et al., 2019).

Most of the carbonaceous chondrite groups are well established and their member meteorites are generally well characterized. A smaller portion of carbonaceous chondrites consists of ungrouped meteorites; they represent ~0.1% of all meteorites as of today. Type 2 ungrouped carbonaceous chondrites (C2-ung) make up an even smaller fraction (~0.04%). Ungrouped carbonaceous chondrites are not easily classified into one of the well-established groups due to compositional/petrological differences and geochemical anomalies (Choe et al., 2010; Cloutis et al., 2012). In general, petrologic type 2 carbonaceous chondrites are known to be moderately aqueously altered and have experienced very little heating (Brearley, 2006). However, complex post-accretionary processes in the parent body(ies) of C2-ung chondrites resulted in a range of anomalous compositional or petrographic properties such that their classification is not straightforward. For instance, Queen Alexandra Range (QUE) 99038 was originally classified as a CM2 chondrite, followed by reclassification as a CV3 chondrite, before being reclassified again as a C2-ung chondrite due to partial similarities as well as clear differences when compared with members of the well-established carbonaceous chondrite groups (Choe et al. [2010]; Meteoritical Bulletin Database [2022] and references therein). Similarly, Elephant Moraine (EET) 83226 was classified as a C2-ung chondrite after initially being classified as a C2 and then a CM2 chondrite (Grady, 2000; MacPherson, 1985; Meteoritical Bulletin Database, 2022). It is also associated with the CV-CK clan and CO3 chondrites on the basis of compositional similarities (Abreu et al., 2018).

Some members of the C2-ung chondrites can potentially represent different aspects of asteroids and their regolith material. They could also be the sole representative of a previously unsampled parent body (Choe et al., 2010; Cloutis et al., 2012). Tagish Lake and Tarda exhibit similar chemical composition to each other and are also classified as C2-ung chondrites, though exhibit very different chemistry, mineralogy, and oxygen isotopic composition than QUE 99038 and EET 83226. Tagish Lake and Tarda are matrix-rich brecciated meteorites with bulk mineralogy that is consistent with being petrologic type 2 chondrites. They are richer in ^{18}O (plotting near the vicinity of CI and CY chondrites, see Fig. 12) and contain abundant carbon and phyllosilicates, and lesser amounts of magnetite, pyrrhotite, and olivine (Brown et al., 2000; Chennaoui Aoudjehane et al., 2021; Nakamura-Messenger et al., 2006; Yesiltas & Kebukawa, 2016; Zolensky et al., 2002). Tagish Lake (Hiroi et al., 2001), Wisconsin Range (WIS) 91600 (Hiroi et al., 2005), and most recently Tarda (Marrocchi et al., 2021) have been proposed to be possible samples from D-type asteroids. Thus, investigation and chemical characterization of C2-ung chondrites can potentially provide invaluable insights into the poorly sampled chondrite parent bodies as well as the range of formation conditions and subsequent histories. They can also shed light on the cosmochemical processes and events that cause such incompatibilities in the C2-ung chondrites and help us differentiate between the secondary processes.

In this work, we present detailed spectroscopic and compositional data on three carbonaceous meteorites that are currently classified as C2-ung chondrites: QUE 99038, EET 83226, and Tarda. Their molecular and elemental compositions were investigated using secondary electron microscopy (SEM), laser ablation inductively coupled plasma mass spectrometry (LA-ICP-MS), and micro-Raman spectroscopy. The available amount of Tarda was large enough to allow further analysis by thermogravimetric analysis (TGA) and Fourier transform infrared (FT-IR) transmission spectroscopy. Two CM2 chondrites and a CV3 chondrite were also measured and compared with the considered C2-ung chondrites.

SAMPLES AND TECHNICAL DETAILS

Samples

QUE 99038 (section #23) and EET 83226 (section #28) were prepared by NASA's Astromaterials Acquisition and Curation Office at Johnson Space Center in the form of polished thin sections. Tarda is a newly recovered sample of an observed fall. A small piece of Tarda was acquired from a private source (D. Dickens) and a polished section was prepared following the same procedures as the QUE 99038 and EET 83226 meteorites. Due to the extremely friable nature of Tarda, it frequently chipped off and plucked during sample preparation. Several pristine (fresh) carbonaceous chondrites, including two CM2s (Aguas Zarcas and Jbilet Winselwan), one CV3 (Allende), and one C2-ung (Tagish Lake), were acquired from private sources (D. Dickens and E. Twelker) for comparison purposes. After breaking off these meteorites, central and previously not exposed parts were removed and prepared as polished sections (except Tagish Lake, which was in the powder form). Table 1 lists the studied meteorites and the utilized analytical techniques.

Table 1. Investigated meteorites and utilized techniques in this work.

Meteorite	Type	Type	SEM	LA-ICP-MS	Raman	FT-IR	TGA
QUE 99038	C2-ung	PS	✓	✓	✓		
EET 83226	C2-ung	PS	✓	✓	✓		
Tarda	C2-ung	PS, chip	✓	✓	✓	✓	✓
Tagish Lake	C2-ung	powder			✓	✓	
Aguas Zarcas	CM2	PS, chip	✓	✓	✓	✓	✓
Jbilet Winselwan	CM2	PS, chip	✓	✓	✓	✓	✓
Allende	CV3	PS, chip	✓	✓	✓	✓	✓

PS = polished section.

Scanning Electron Microscopy

Backscattered electron (BSE) images of the polished sections of QUE 99038, EET 83226, and Tarda were acquired using a Zeiss EVO 10L secondary electron microscope with an X-ray detector at Trakya University. Measurements were conducted at 15 kV with a beam current of 5 nA. Individual BSE images were then stitched to create the full mosaic image for each meteorite. Energy-dispersive X-ray spectroscopic (SEM-EDS) data for Ca and Si, as internal standards for the LA-ICP-MS measurements, were collected (at a separate session) at 15 kV with a beam current of 5 nA using an EDX detector (Oxford XACT) mounted on a Hitachi SU3500 T2 model scanning electron microscope. The acquired SEM-EDS data were analyzed using the Oxford XACT instrument software package.

Micro-Raman Spectroscopy

Micro-Raman spectroscopic measurements were conducted on polished meteorite sections over a spectral range of 0–4000 cm^{-1} using a commercial confocal Raman imaging system (WiTec alpha300R) at Gazi University. The system is equipped with 600 grooves per mm grating, 532 nm Nd:YAG laser, and 50× objective (NA = 0.8). The spectrograph was calibrated using a silicon wafer substrate prior to measurements. The power density of the circular ~0.8 μm diameter laser beam was ~0.5 to 1 mW μm^{-2} on the sample surface throughout the data acquisition. Individual Raman spectra were collected for 60 accumulations with 1 s integration time. Two-dimensional Raman intensity maps of 50 × 50 or 100 × 100 μm^2 sizes were collected with a 0.5 μm step size (pixel size) with the same laser power density and 0.1–0.3 s integration time. These parameters did not cause artificial modification of the carbonaceous matter and no systematic shift in the spectral parameters (such as peak widths or positions) were observed when multiple laser shots were directed to the same spot (e.g., Yesiltas et al., 2018, 2019, 2020). After collecting data in the matrices of meteorites, intensity distribution maps of individual chemical components were generated by integrating the signal between the spectral endpoints of Raman peaks using a commercial software package (WITec Project). Data reduction procedures include cropping the Rayleigh laser line, removing cosmic rays and artificial baseline (by subtracting a polynomial with shape size of 200 and noise factor of 2), fitting the first-order (and second-order, when available) carbon peaks with Lorentzian functions, and finally extracting spectral parameters full-width-half-maxima (Γ), intensity (I), and position (ω) of the carbon peaks (Fig. 1).

Laser Ablation Inductively Coupled Plasma Mass Spectrometry

Chemical analyses were performed on polished meteorite sections after the nondestructive analyses were completed. We used a Perkin Elmer NexION 2000 mass spectrometer and an ESI NWR-213 solid-state laser ablation system at Istanbul University-Cerrahpasa for collecting the compositional data. LA-ICP-MS measurements were carried out in dual detector (pulse and analog counting) mode with 10 ms dwell time for the isotopes listed in the supporting information document. Isotopes with the least interference were selected for analysis according to Syngistix for ICP-MS v.2.3 software package for most trace elements. During instrument calibration, the ThO/Th ratio was set to <0.05% and ^{238}U cps >100,000. Data from a total of 30 points were collected from the matrices of considered meteorites, where the crater size was ~50 μm, and the crater depth was ~15 μm. Energy level of 5J and repetition rate of 5 Hz were maintained throughout the measurements. NIST SRM610 and SRM612 standards (Pearce et al., 1997) were measured as primary references, and BCR-2g (Jochum et al., 2005) was used as a secondary reference. During the measurements, 30 s of gas blank, 30 s of ablation time, and 20 s of washout times were selected. He (0.6 l s^{-1}) was used as the carrier gas. Data reduction was carried out using the ICPMSDATACALL (Liu et al., 2008) software package.

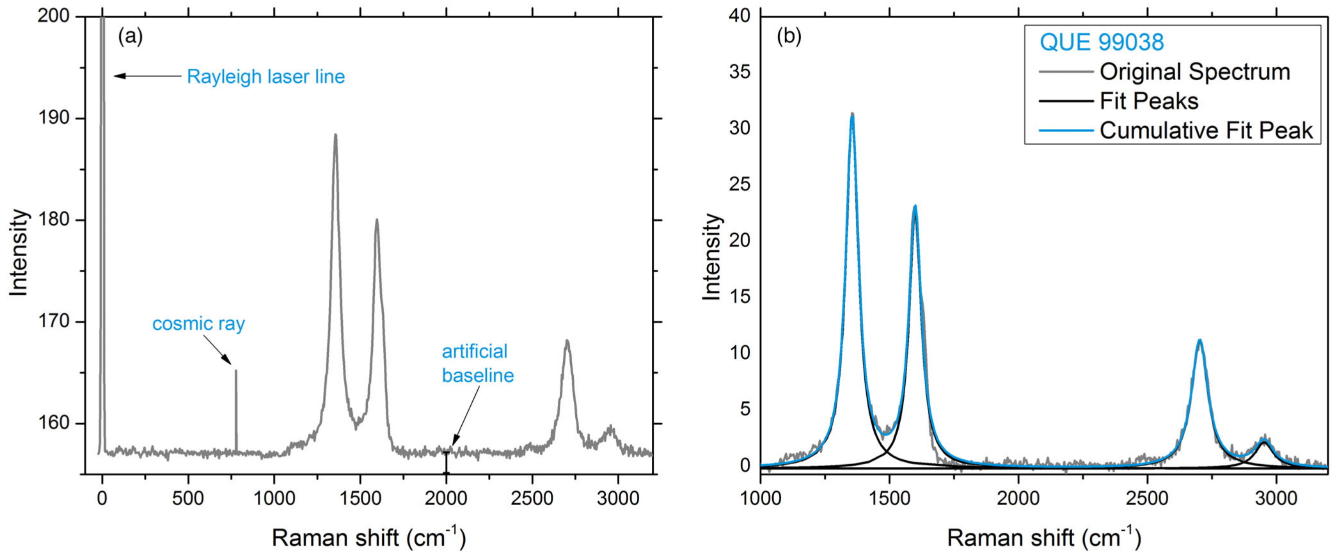

Fig. 1. Example of raw (a) and processed (b) Raman spectrum of carbonaceous matter in QUE 99038. Processing a Raman spectrum includes the removal of the Rayleigh laser line, cosmic rays, and fluorescence-induced background.

Mid-Infrared Transmission Spectroscopy

FT-IR transmission spectral data were collected on two C2-ung chondrites (Tarda and Tagish Lake) as well as three other carbonaceous chondrites (Aguas Zarcas, Jbilet Winselwan, and Allende) to identify and compare their mineralogical content and hydrated phases. A small chip of each meteorite was broken off the main chip and subsequently ground in a mortar and pestle set down to 10–50 µm sized powder; 12.5 mm diameter pellets were made for each meteorite by mixing ~1.5 mg meteorite powder and ~400 mg of KBr. Mid-infrared (4000–400 cm^{-1}, 2.5–25 µm) transmission spectra were collected at Bilkent University with 4 cm^{-1} spectral resolution using a Nicolet 6700 (Thermo Fisher Scientific) FT-IR system. The samples were heated at 200 °C for 1.5 h in order to eliminate the adsorbed water. We note that some of the adsorbed water may have reentered the sample between the oven and the FT-IR instrument even though the exposure was only a few minutes.

Thermogravimetric Analyses

Small portions (10–15 mg) of the powdered meteorites, Tarda, Aguas Zarcas, Jbilet Winselwan, and Allende, were used to conduct TGA at Bilkent University in an effort to determine and compare their state of hydration. We used a Q500 (TA Instruments) thermal analyzer for performing the TGA. Powder of each meteorite was placed in an alumina crucible for measurements, and heated from 25 to 950 °C at a continuous heating rate of 10 °C min^{-1} in a nitrogen gas atmosphere flowing at 60 ml min^{-1}. Each meteorite was measured three times for reproducibility of the TGA data, which yielded ~0.25% error on the mass loss and ~0.20 °C on the temperature readings.

RESULTS

Petrology and Chemical Composition

Mosaic and individual BSE images of QUE 99038 are shown in Fig. 2a–m. These images show the presence of coarse-grained matrix, Fe-rich rims on olivines, and apparent lack of tochilinite, suggesting lack of aqueous alteration and/or exposure to metamorphism for QUE 99038. EET 83226 is a clastic carbonaceous chondrite with high porosity. BSE images in Fig. 3a–i show that it consists of numerous large chondrules with ~30–100 µm thick fine-grained rims (FGRs) set within fine-grained matrix. Some FGRs are highly fragmented and discontinuous (e.g., Fig. 3e and 3g).

Fig. 2. BSE mosaic image of QUE 99038 (a) as well as images of various chondrules, matrix, and opaque phases (b–m). b, c) Olivine chondrules with Fe-Ni and FeS blobs. d) Olivine chondrule with roughly circularly distributed pyroxene separating the olivine core. e, f) Metal-rich olivine chondrule. g) Barred olivine chondrule. Bars exhibit two orientations in the upper and lower parts of the chondrule. h) Coarse-grained nature of the matrix. i–k) Fe-Ni and FeS within an olivine chondrule. l) Barred olivine chondrule. m) Coarse olivine–pyroxene particles within the matrix. Black scale bars are 200 µm.

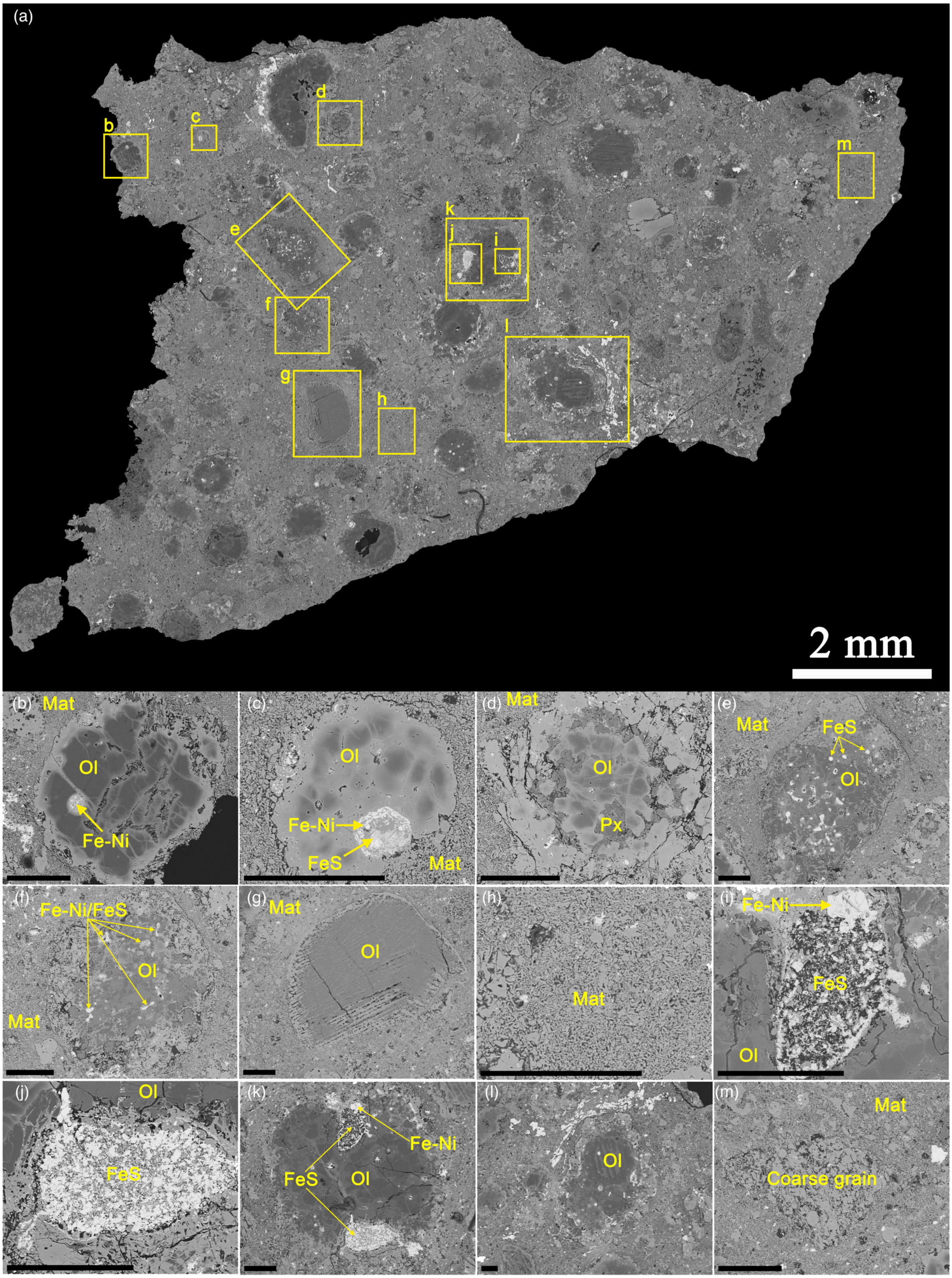
(a)
b
c
d
e
f
g
h
i
j
k
l
m
2 mm
(b) Mat
Ol
Fe-Ni
(c)
Ol
Fe-Ni
FeS
Mat
(d) Mat
Ol
Px
(e)
Mat
FeS
Ol
(f)
Fe-Ni/FeS
Ol
Mat
(g) Mat
Ol
(h)
Mat
(i) Fe-Ni
FeS
Ol
(j) Ol
FeS
(k)
Fe-Ni
FeS
Ol
(l)
Ol
(m)
Mat
Coarse grain

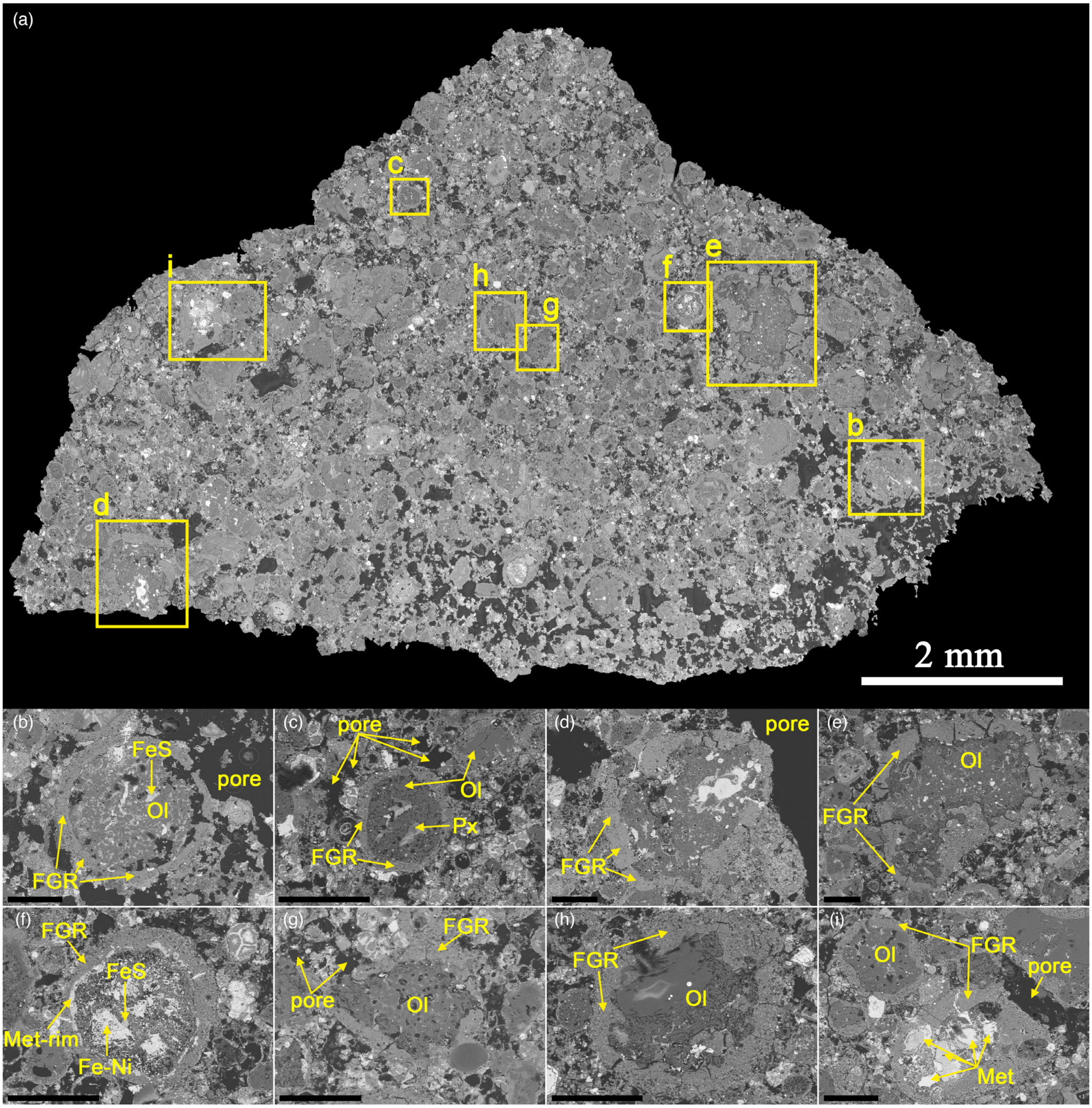

Fig. 3. BSE mosaic image of EET 83226 (a) as well as images of various rimmed chondrules, matrix, and opaque phases (b–i). b) Olivine chondrule with FGR and FeS phases inside. Dark gray regions are pores. c) Rimmed olivine chondrule with pyroxene. d, e) Metal-rich olivine chondrules with thick and fragmented FGRs. f) Olivine chondrule containing Fe-Ni and FeS as well as metal-rich rim, enclosed by FGR. g, h) Olivine chondrules with fragmented and discontinuous FGRs, which are often the case in EET 83226. i) Rimmed olivine chondrule above metallic phases. Black scale bars are 200 μm.

Observed metal phases include Fe-Ni, FeS, and chromite. Figure 4a–g presents BSE images of Tarda. This meteorite is highly friable, and small bits and pieces of it plucked during the sample preparation, resulting in holes on the surface of the sample. Tarda contains different types of chondrules (some with Fe-rich rims), framboid magnetite, sulfides, phyllosilicate- and carbon-rich matrix. Organic matter and phyllosilicates are also found within dark clasts set in the matrix.

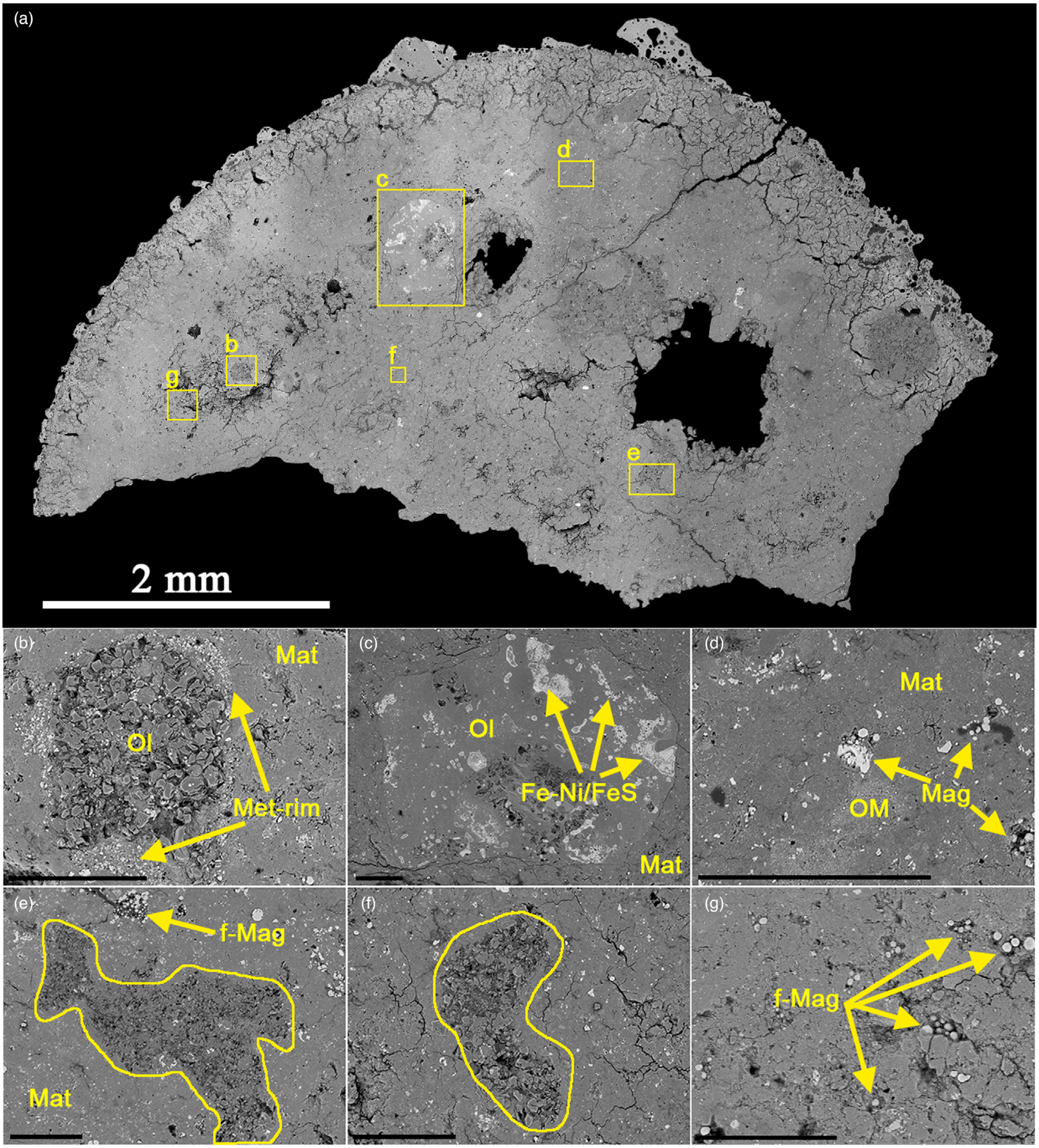

Fig. 4. BSE mosaic image of Tarda (a) and images of various chondrules, matrix, and opaque phases (b–g). b) Granular olivine chondrule with metal-rich rim. c) Olivine chondrule with Fe-Ni and FeS blobs scattered within the chondrule. d) Magnetite particles and organic matter-rich phase set within the matrix. e, f) Darker color granular clasts and magnetite framboids. g) Magnetite framboids within the matrix. Black scale bars are 100 μm.

Major oxide abundances of the matrix of studied meteorites collected by LA-ICP-MS are given in Table 2. QUE 99038 has the highest Al_2O_3 and CaO among the studied samples, suggesting the presence of plagioclase. This is supported by the presence of Na in the composition of QUE 99038. MgO and CaO in QUE

Table 2. Matrix composition (wt%) of meteorites.

Major oxides	QUE 99038	EET 83226	Tarda	Aguas Zarcas	Jbilet Winselwan	Allende	CM2 avg	CO3 avg	CV3 avg	C2un avg
SiO_2	41.17	43.13	34.04	31.91	35.40	31.97	27.66	27.75	29.98	24.57
Al_2O_3	8.72	4.16	2.80	0.10	0.08	0.09	2.57	3.12	3.11	3.03
TiO_2	0.38	0.12	0.12	2.14	2.40	1.72	0.06	0.09	0.08	0.06
FeO	11.93	25.08	27.26	36.21	32.98	35.37	31.01	32.57	35.04	30.61
MnO	0.12	0.18	0.18	0.27	0.24	0.21	0.20	0.19	0.20	0.17
MgO	27.14	20.42	29.76	21.20	22.53	22.44	16.42	19.15	21.00	14.28
CaO	7.44	2.06	0.78	2.45	0.94	2.80	0.54	1.00	1.21	1.12
Na_2O	1.51	1.87	0.53	0.50	0.70	0.11	0.50	0.24	0.43	0.55
P_2O_5	0.10	0.40	0.37	0.32	0.05	0.04	0.24	0.15	0.57	0.24
K_2O	0.18	0.08	0.10	0.14	0.14	0.01	0.08	0.04	0.05	0.16
Total	98.69	97.5	95.94	95.24	95.46	94.76	79.28	84.3	91.67	74.79

CM2 (Murchison, Nogoya, Mighei, Murray), CO3 (Warrenton, Felix), CV3 (Allende, Vigarano, Bali, Kaba), and C-ung (Essebi, MAC87300) data are average microprobe matrix compositions from Zolensky et al. (1993).

99038 suggest the presence of anhydrous silicates such as olivine and pyroxene. It also has the lowest matrix FeO. The C2-ung chondrites QUE 99038, EET 83226, and Tarda have lower TiO_2 and FeO but higher Al_2O_3 in their respective matrices than those of other chondrites. Major oxide abundance as well as CI (McDonough & Sun, 1995) and Yb normalized trace and REE elemental composition of the matrix of studied meteorites are given in Fig. 5. Average matrix composition of CM2, CO3, CV3, and C-ung chondrites from the literature (Bland et al., 2005; Kallemeyn & Wasson, 1981; Kong & Palme, 1999; Rubin & Wasson, 1987, 1988) is also plotted along with our samples for comparison. Trace element composition of QUE 99038 appears different than the rest of the samples and groups. It has the lowest Sc, V, Co, Ni, Ga, Ge, Y, Zr, Cs, Hf, and Pb (Fig. 5b). It is especially relatively depleted in Co, Ni, Ga, and Ge. EET 83226 exhibits slightly lower trace element composition as well. It has the second lowest Sc, V, Co, and Ni values. The trace element composition of Tarda appears very similar to those of C-ung chondrites (except for Sr). Aguas Zarcas and Jbilet Winselwan exhibit very little variation in their matrix trace element composition and are comparable to average CM2 chondrites. Tarda exhibits a similar matrix REE composition to average CM2, CO3, CV3, and C-ung chondrite values, which have flat and similar matrix REE compositions (Fig. 5c). Other meteorites we considered have slightly higher La, Ce, and Nd values. QUE 99038 has the lowest Ho, Er, and Lu values, while EET 83226 has the lowest Gd, Tb, and Dy values. We note that abundances of Co and Ni given in Table S2 in supporting information appear to be large, which could be due to the variations in the metal content of a measured spot in the respective matrices of studied meteorites.

Thermal Metamorphic History

Visible micrographs and Raman spectra of polyaromatic organic matter in QUE 99038, EET 83226, and Tarda are presented in Fig. 6. Figure 6f also presents a Raman spectrum of Tagish Lake (carbonate-rich lithology) for comparison. The polyaromatic organic matter appears to be present within the matrix, often homogeneously distributed of all four C2-ung chondrites (Fig. 6a and 6d–f). Their Raman spectra display well-developed first-order D (disorder) and G (graphite) carbon bands centered, respectively, at ~1350 and ~1590 cm^{-1} (Fig. 6c and 6g). These first-order bands are due to sp2 and sp3 carbon bonding (Ferrari & Robertson, 2000). Aguas Zarcas, Jbilet Winselwan, and Allende similarly present such first-order carbon bands as well. The second-order Raman carbon bands, 2D band at ~2700 cm^{-1}, and D + G band at ~2930 cm^{-1} are overtones of the first-order bands. QUE 99038 and Allende are the only chondrites in this work that present these second-order bands (Fig. S1 in supporting information).

Thermal metamorphic grade of samples can be estimated to some extent through the comparison of Raman carbon band properties (such as ω, I, and Γ), as Raman spectroscopy is sensitive to degree of disorder in carbon structures (Beyssac et al., 2002, 2003; Casiraghi et al., 2005). Raman parameters of the first-order carbon bands show that the D band of QUE 99038 is the narrowest among all meteorites considered in this work, and plot in close proximity to CV3 (average of 12) chondrites (Fig. 7a). This band is relatively broader in EET 83226 and even broader in Tarda. The increasing G band position with decreasing width (Γ) is indicative of increasing thermal metamorphism (Busemann et al., 2007), and QUE 99038 plots near the lower right corner of Fig. 7b where CV3 chondrites

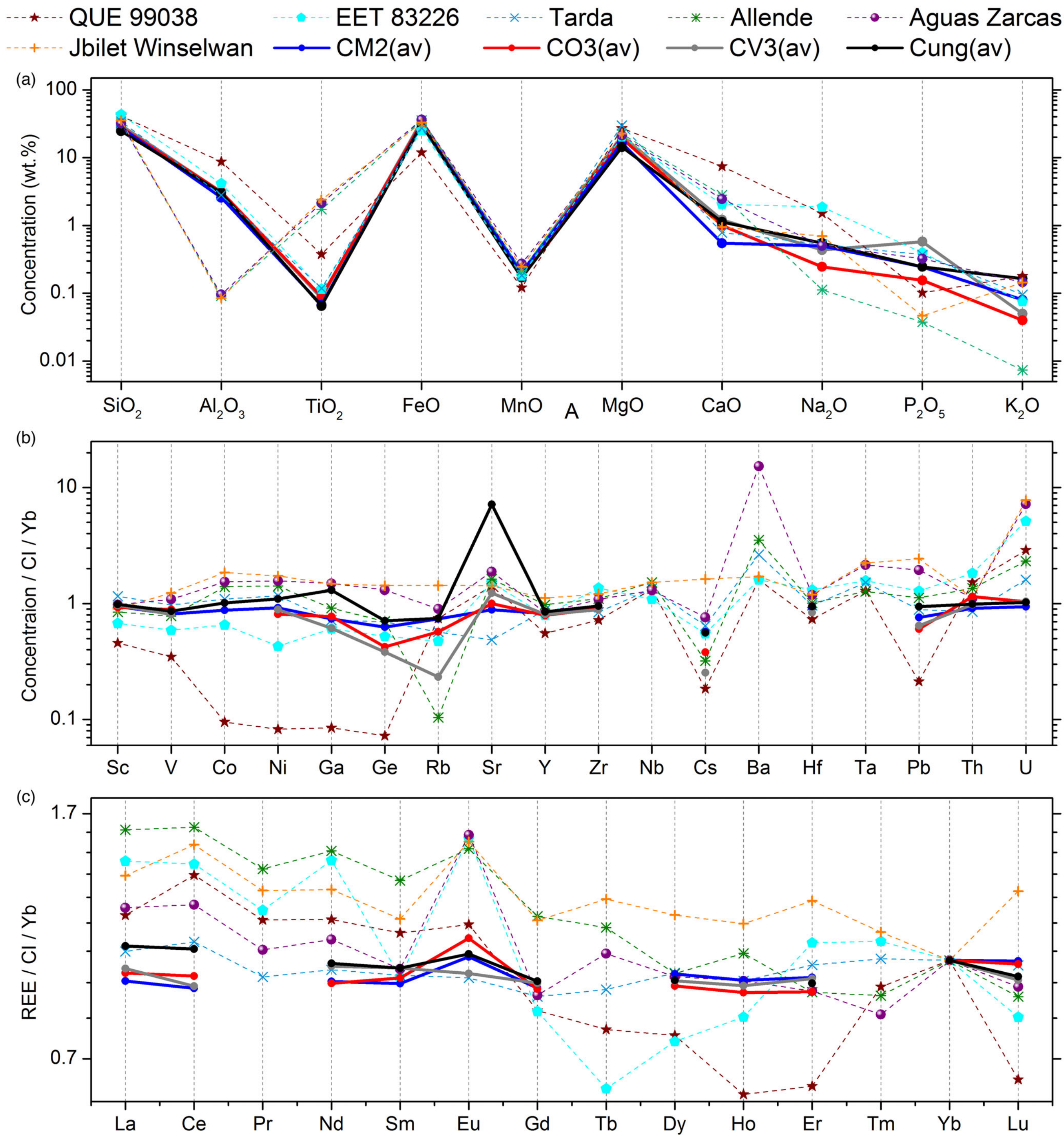

Fig. 5. Major (a) as well as CI and Yb normalized trace (b) and REE (c) elemental composition of the matrix of studied meteorites determined by LA-ICP-MS (dashed lines). Average matrix data for CM2, CO3, CV3, and C-ung chondrites (solid lines) in (a) are from Zolensky et al. (1993), and those in (b, c) are from Rubin and Wasson (1987, 1988), Kong and Palme (1999), Kallemeyn and Wasson (1981), and Bland et al. (2005).

plot. Figure 7c presents a comparison of intensity ratio I_D/I_G with D band width (Γ_D). In this graph, the data were fit with a cubic function (gray line), which is roughly representative of increasing thermal metamorphism. The I_D/I_G ratio of QUE 99038 (1.30 ± 0.06) is one of the highest and plots near the

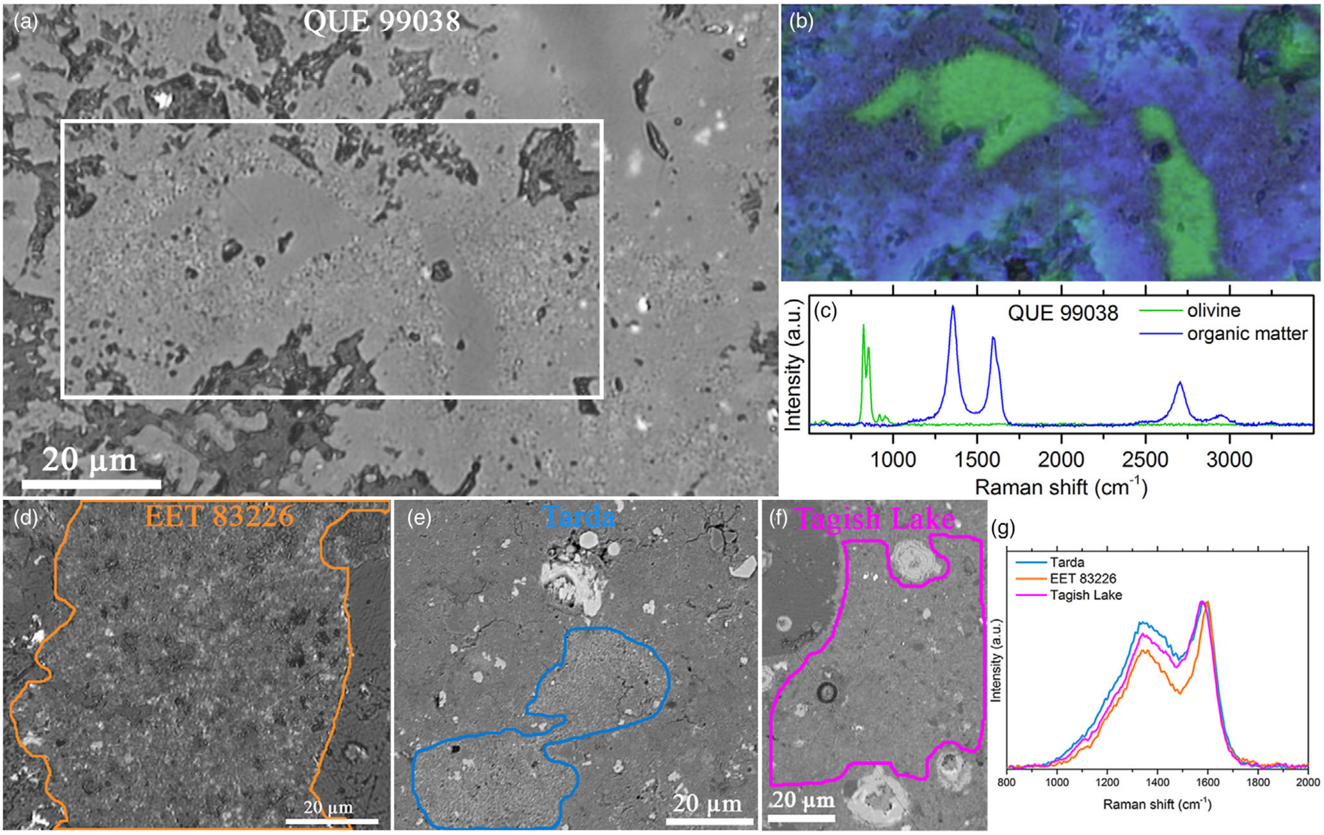

Fig. 6. Visible micrographs and corresponding Raman spectra of the studied C2-ung chondrites. a) Studied region in QUE 99038. White rectangle indicates the location of a macromolecular carbon-rich area. b, c) Intensity distribution map and corresponding Raman spectra of carbon (blue) and olivine (green) present within the white rectangle shown in (a). d–f) Visible micrographs of EET 83226, Tarda, and Tagish Lake. Carbon-rich matrices are indicated by orange, blue, and pink lines, respectively. g) Raman spectra of EET 83226, Tarda, and Tagish Lake.

CV3 chondrites on the left end of the gray line where the effect of metamorphism is the highest. Tarda has an I_D/I_G ratio of 1.00 ± 0.12 and plots on the opposite end of the gray line, along with Tagish Lake (C2-ung), which indicates Tarda and Tagish Lake experienced much less thermal metamorphism than QUE 99038. EET 83226 has the lowest I_D/I_G ratio (0.77 ± 0.05) and plots close to CO3 chondrites and Aguas Zarcas (CM2), which can be indicative of moderate thermal metamorphism. Furthermore, a linear trend is observed when the width ratio Γ_D/Γ_G is compared with the width of D band (Γ_D) in Fig. 7d. QUE 99038 again plots near the CV3 chondrites at the lowest part of the trend, while EET 83226 plots near the middle and close to CO3 (average of 12) chondrites. Tarda and Tagish Lake plot near the top of the trend line, where aqueously altered and less thermally metamorphosed meteorites plot. In this context, Raman spectral parameters of QUE 99038 are quite different than other C2-ung chondrites. In fact, it looks very similar to Allende, which is an oxidized CV3 chondrite.

State of Hydration

Mid-infrared FT-IR spectra can be useful for the characterization of chemical composition of carbonaceous chondrites (e.g., Bates et al., 2020, 2021; Kebukawa, Alexander, et al., 2019; Kebukawa, Ito, et al., 2019; Kebukawa et al., 2020; King et al., 2015, 2019; King, Schofield, et al., 2021; Miyamoto & Zolensky, 1994; Morlok et al., 2020; Potin et al., 2020; Takir et al., 2013, 2019; Yesiltas, Glotch, & Kaya, 2021; Yesiltas, Glotch, & Sava, 2021; Yesiltas et al., 2017). Figure 8a presents mid-infrared spectra of Tarda, Tagish Lake, Aguas Zarcas, Jbilet Winselwan, and Allende together with spectra of other carbonaceous chondrites from Kebukawa, Alexander, et al. (2019). All meteorites contain hydration bands; a broad band between 3750 and 3000 cm^{-1} due to O-H stretching vibrational modes of adsorbed and/or interlayer water in phyllosilicates, a weak but sharp accompanying feature at 3680 cm^{-1} due to structural OH, and a band centered at 1630 cm^{-1} due to the fundamental H-O-H

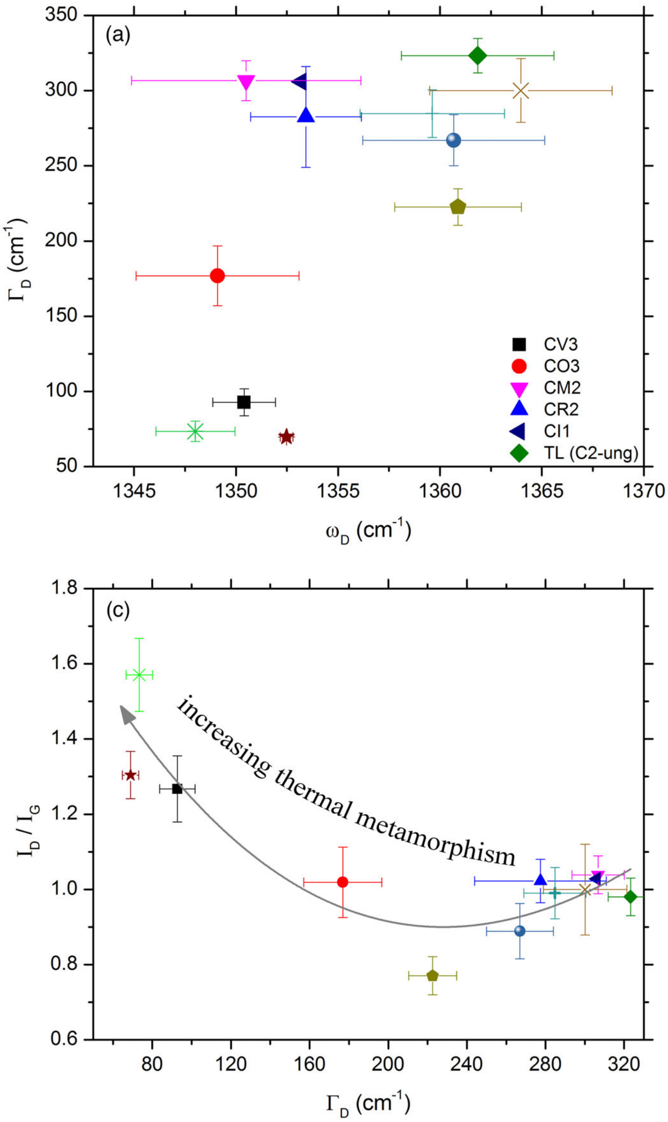

Fig. 7. Raman spectral band properties of carbon in the studied carbonaceous chondrites compared to those of C chondrites from well-established groups. Comparison of Γ_D (a) shows that thermally metamorphosed meteorites have narrower width. Comparison of Γ_G with G band position (b) shows a linear trend for increasing thermal metamorphism. The I_D/I_G (c) and Γ_D/Γ_G (d) ratios, when compared with Γ_D, also show a trend where thermally metamorphosed meteorites plot at the opposite end of more primitive meteorites. Average CV3 (black, $n = 12$) and CO3 (red, $n = 12$) data are from Yesiltas, Young, et al. (2021). Average CM2 (pink, $n = 6$), CR2 (blue, $n = 7$), and CI1 (dark blue, $n = 1$) data are from Busemann et al. (2007).

bending mode in adsorbed and/or interlayer water. These bands are relatively weaker in the case of Allende and Kaba due to their metamorphosed nature and lack of phyllosilicates. All meteorites present small features between 3000 and 2800 cm^{-1}, diagnostic of aliphatic hydrocarbons. This region is enlarged in Fig. 8b to show individual peaks. The peaks at ~2920 and ~2850 cm^{-1} are due to CH_2 moieties, while those at ~2960 and 2875 cm^{-1} are due to CH_3 moieties. The carbonate peak is centered around 1430 cm^{-1} and is present in most meteorites, although it is the strongest in Tarda and Tagish Lake. This is indicative of the presence of abundant carbonates in the composition of Tarda and Tagish Lake. The strong band at 1010 cm^{-1}, characteristic of SiO_4 stretching in phyllosilicates, indicates that most meteorites presented here contain abundant phyllosilicates, except Allende, which instead presents a stronger olivine peak near 880 cm^{-1}. This peak is correlated with another olivine peak at 505 cm^{-1}. Bulk FT-IR spectra of QUE 99038 and EET 83226 could not be collected in this work due to insufficient amounts of samples. However, reflectance spectra of powdered QUE 99038 (Takir et al., 2013) and EET 83226 (Takir et al., 2019) present weak 3 μm

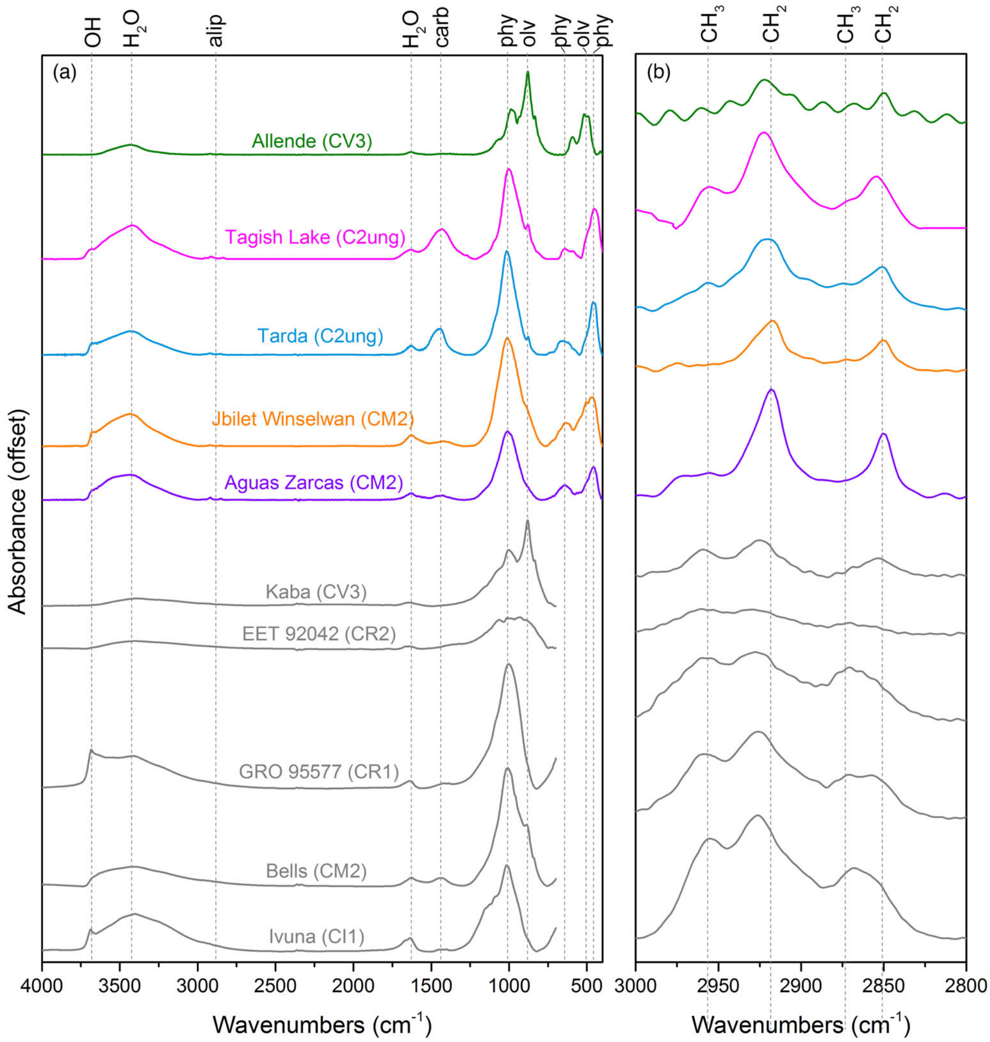

Fig. 8. FT-IR transmission spectra of carbonaceous chondrites (a). Gray spectra are from Kebukawa, Alexander, et al. (2019) and plotted together with the meteorites studied in this work for comparison. The vertical dashed lines indicate positions of identified hydration bands (OH, H_2O), aliphatic hydrocarbons (alip), carbonates (carb), phyllosilicates (phy), olivines (olv). The 3000–2800 cm^{-1} region is expanded, respectively, in (b) to reveal the aliphatic C-H features.

OH band (band centers at 2.7 and 2.83 μm, or 3700 and 3533 cm^{-1}, respectively), and QUE 99038 additionally exhibits infrared features at 1 and 2 μm, diagnostic of anhydrous silicates including olivine and pyroxene. Such near-infrared bands of anhydrous silicates are absent in that of EET 83226.

The endogenous water content of carbonaceous chondrites includes molecular water, interlayer water, structural OH, and water in micropores (Dubinin, 1980; Garenne et al., 2014; King et al., 2015; King, Schofield, et al., 2021). ++TGA allows the characterization of water as it measures the mass (or mass loss %) of a sample as a function of sample temperature (Bottom, 2008; Garenne et al., 2014; King et al., 2015; King, Schofield, et al., 2021). Each mass loss fraction is due to release of a specific type of hydration and breakdown of carbonates, organic matter, sulfides, etc., and thus, different temperature ranges can be attributed to different types of released H_2O or OH and breakdown of components (Garenne et al., 2014; King et al., 2015). Namely, 25–200 °C, 200–400 °C, 400–700 °C, and 700–900 °C temperature ranges are, respectively, due to absorbed molecular water, hydroxides/organics, phyllosilicates, and carbonates (Garenne et al., 2014; Gilmour et al., 2019; King et al., 2015). It's worth noting that these ranges can vary depending on the chemical composition of different meteorites, as previously shown. Depending on the type of phyllosilicate minerals in the meteorites, the temperate range for the dehydration of phyllosilicates can be generally taken as 400–700 °C (e.g., Che & Glotch, 2012; Che et al., 2011; Gilmour et al., 2019) or wider such as 400–770 °C (Garenne

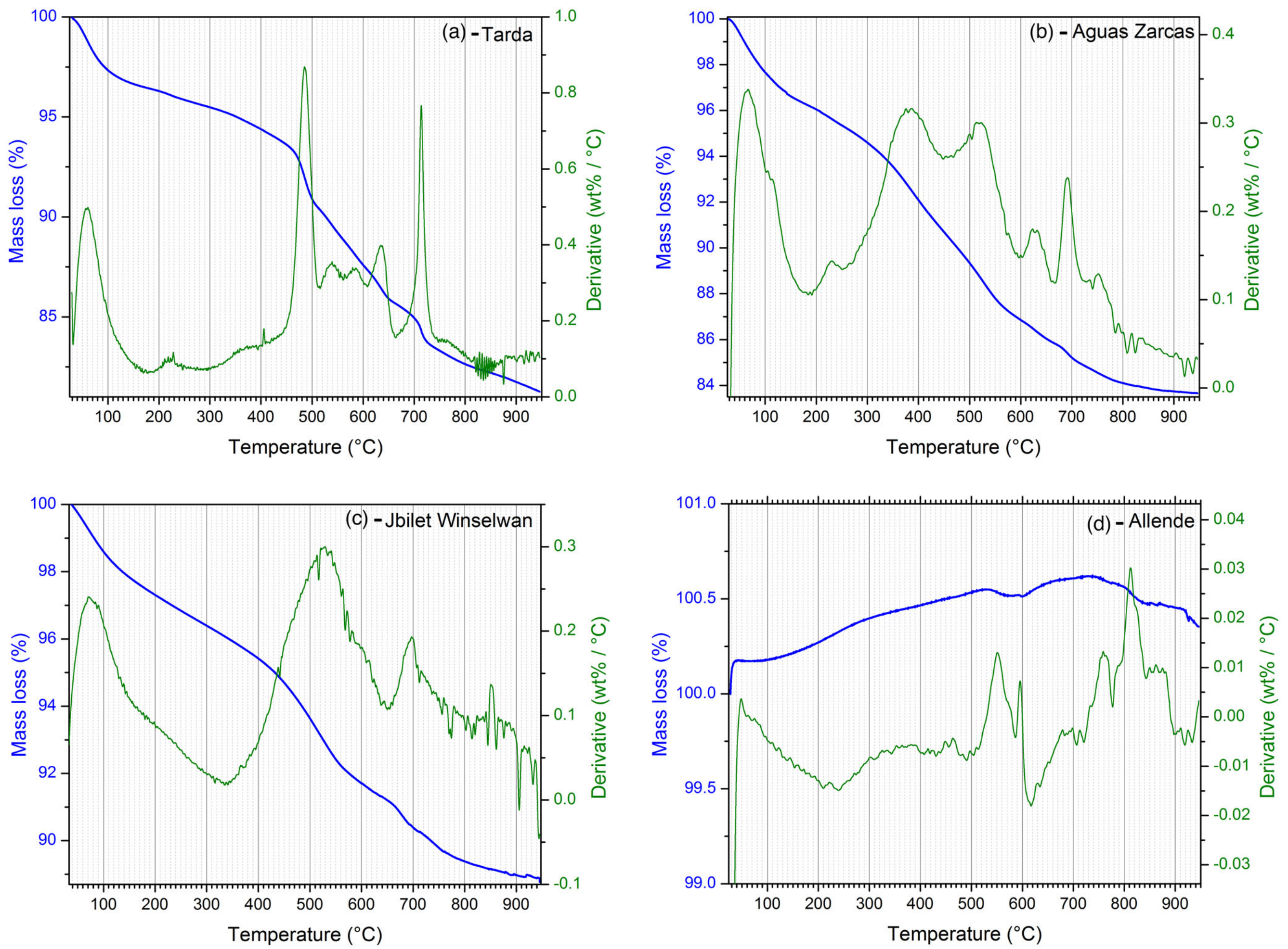

Fig. 9. TGA and derivative curves for (a) Tarda, (b) Aguas Zarcas, (c) Jbilet Winselwan, and (d) Allende from 25 to 950 °C.

et al., 2014) in the case of phyllosilicate-rich samples. It can even be taken as 300–800 °C if smectites are present (King et al., 2015).

When combined with IR spectra, TGA data can be used to examine the bulk mineralogy and hydration content of carbonaceous chondrites and useful insights into their respective aqueous alteration histories can be gained (Garenne et al., 2014; King et al., 2015; Potin et al., 2020). The first derivative of the TGA curve allows monitoring the rate of change in the mass of the sample during the heating cycle. Thus, its peaks can be associated with different organic/inorganic phases. By examining the mass loss events in the TGA spectra, it seems plausible to use the 25–200 °C, 200–400 °C, 400–700 °C, and 700–900 °C temperature ranges for the absorbed molecular water, hydroxides/organics, phyllosilicates, and carbonates, respectively. In this work, Tarda, Aguas Zarcas, Jbilet Winselwan, and Allende were gradually heated from 25 to 950 °C while the mass of the sample was measured throughout the experiment. Figure 9 presents the mass loss (wt%) as well as derivative (wt% per °C) curves of meteorites with respect to temperature, while Fig. 10 compares the mass loss percentages for different meteorites. In Tarda, molecular water is responsible for 3.70 wt% mass loss; hydroxide and oxyhydroxide minerals are responsible for 1.90 wt% mass loss; dehydration of phyllosilicates results in 9.45 wt% mass loss; and decomposition of carbonates results in 3.20 wt% mass loss, totaling ~18.25 wt% mass loss. Tarda's total mass loss as well as the mass loss due to individual components are very similar to Tagish Lake (Table 3). Aguas Zarcas (CM2) experienced a total mass loss of 16.27 wt%, out of which 3.95 wt% is due to molecular water, 3.96 wt% is due to hydroxide and oxyhydroxide minerals, 6.88 wt% is due to phyllosilicates, and 1.48 wt% is due to carbonates. The dehydrated CM2 chondrite Jbilet Winselwan experienced a total mass loss of 11.03 wt%.

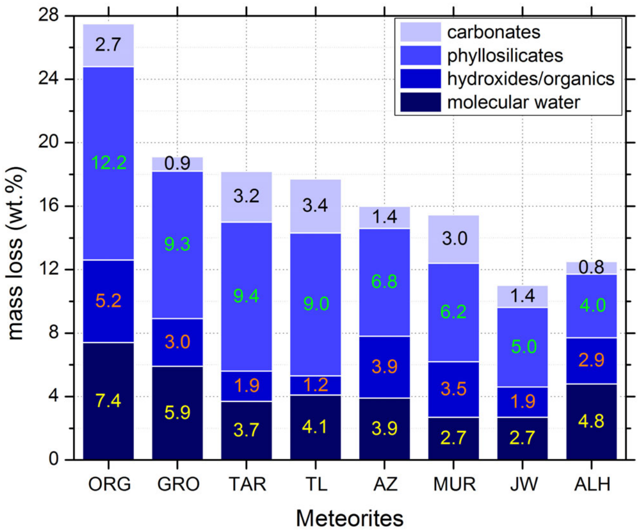

Fig. 10. Comparison of TGA mass loss fractions (wt%). Orgueil (Org, CI1), GRO 95577 (GRO, CR1), Tagish Lake (TL, C2-ung), ALH 84033 (ALH, CM2), and recalculated Murchison (Mur, CM2) data are from Garenne et al. (2014).

Roughly 2.68 wt% is due to molecular water, 1.89 wt% is due to hydroxide and oxyhydroxide minerals, 5.03 wt% is due to phyllosilicates, and 1.42 wt% is due to carbonates. In this context, Jbilet Winselwan appears to have fewer phyllosilicates and carbonates relative to Tarda and Tagish Lake. It's worth noting that Aguas Zarcas contains different lithologies, such as C1 and C1/2 (Kerraouch et al., 2021), though the sample studied in this work did not appear to contain those lithologies and exhibited CM2 textures. Orgueil presents the highest phyllosilicate abundance and the highest total mass loss between 200 and 800 °C (not including 25–200 °C, which is due to the terrestrial adsorbed water and weathering products). The hydration state of Allende cannot be easily investigated due to the increased mass during the measurements. The increase of the mass instead of decrease is counterintuitive because the sample is expected to lose mass due to decomposition of volatiles. However, some carbonaceous chondrites, especially those with abundant chondrules with distinct chondrule mineralogy, appear to gain mass over the temperature ranges instead of losing it (Garenne et al., 2014). Such mass gain indicates that the abundance of hydrated phases is very low, and is likely due to the formation of sulfides and/or metal. At any case, the mass gain prevents the investigation of Allende's state of hydration via TGA. Mass loss percentages are collected in Table 3, except for QUE 99038 and EET 83226 because of insufficient meteorite samples.

DISCUSSION

QUE 99038 Contains CV3$_{oxA}$-Like PAHs

QUE 99038 was originally classified as a CM chondrite based on the preliminary investigations; however, existence of certain differences was later recognized. Initial examinations showed that QUE 99038 contains $Fa_{1\text{-}39}$ and <0.1 vol% metallic Fe-Ni (Grossman & Zipfel, 2001; McBride et al., 2001). It also contains abundant chondrules (~590 μm) and mineral grains set in a black/dark gray matrix (Choe et al., 2010; Grossman & Zipfel, 2001; McBride et al., 2001). Takir et al. (2013) reported that QUE 99038 is a significantly aqueously altered CM2.4 chondrite, and its infrared spectra present the 3 μm band due to OH, indicating the presence of hydrated phases. Chondrules in QUE 99038 are larger than those in CM (270 μm; Huber et al., 2006), and its reflectance spectra appear different than most CM chondrites (Cloutis et al., 2012). Due to these dissimilarities with the CM class, abundant calcium-aluminum-rich inclusions, and a small amount of matrix, QUE 99038 was reclassified as a CV3 chondrite (e.g., Ruzicka et al., 2015). The chondrule sizes in QUE 99038 (~590 μm) are much larger than CM chondrites (~270 μm), smaller than those of CV chondrites (~910 μm), and are more similar to those of CR chondrites (~700 μm); however, there is much less metals in QUE 99038 (i.e., <0.1 vol% metallic Fe-Ni) with respect to CR chondrites (Choe et al., 2010). Refractory lithophile elements and infrared reflectance spectra of QUE 99038 appear to be similar to those of CO chondrites (Cloutis et al., 2012; Huber et al., 2006). Moreover, oxygen isotopic composition of QUE 99038 plots below the carbonaceous chondrite anyhdrous mineral (CCAM) line, which is indicative of being depleted in H_2O (Choe et al. [2010] and references therein). As a result of its complex and anomalous composition and petrographic properties, QUE 99038 was reclassified one more time, into C2-ung chondrite group (Choe et al., 2010; Huber et al., 2006).

It is clear that QUE 99038 is a unique meteorite with complex composition. Despite the latest classification as C2-ung chondrite by Choe et al. (2010), our investigation suggests it is rather an anhydrous chondrite, possibly a petrologic type 3. It also presents almost exactly the same MgO and CaO (likely in anhydrous silicates) contents as in Allende (Fig. 5a). Furthermore, unpublished TGA and X-ray powder diffraction data collected on another piece of QUE 99038 indicate that it is an anhydrous meteorite containing abundant olivine and pyroxene (Ashley King, personal communication), which is in agreement

Table 3. TGA weight loss (wt%) of meteorites with respect to temperature ranges.

Meteorite	Type	25–200 °C (molecular water)	200–400 °C (hydroxides or organics)	400–700 °C (phyllosilicates)	700–900 °C (carbonates)	Total weight loss (wt%)
Tarda	C2-ung	3.70	1.90	9.45	3.20	18.25
Tagish Lake[a]	C2-ung	4.10	1.25	9.05	3.45	17.85
Aguas Zarcas	CM2	3.95	3.96	6.88	1.48	16.27
Jbilet Winselwan	CM2[e]	2.69	1.89	5.03	1.42	11.03
Murchison[b,c]	CM2	2.70	3.50	6.23	3.06	15.49
ALH 84033[c]	CM2[e]	4.70	2.90	3.50	1.25	12.33
GRO 95577[b,d]	CR1	5.90	3.00	9.30	0.90	19.10
Orgueil[b,d]	CI1	7.40	5.20	12.20	2.70	27.50

[a]Average of specimen TL11i from Gilmour et al. (2019).
[b]From Garenne et al. (2014).
[c]Recalculated.
[d]Between 400 and 770 °C.
[e]Heated.

with our observations. Near-infrared spectrum of QUE 99038 resembles type 3 chondrites more than type 2 chondrites (e.g., Cloutis et al., 2012). Petrographic and spectroscopic observations presented here somewhat differ from some of the previously reports in the literature (e.g., Choe et al., 2010; Takir et al., 2013). For instance, in addition to observing the 3 µm OH band, Takir et al. (2013) identified altered chondrule mesostasis, poorly characterized phases/clumps, matrix serpentines, and tochilinite in QUE 99038, hence classifying it as a significantly altered CM2.4 chondrite. However, the observed OH band is weak and shallow, and the abundance of hydrated phases is rather low, indicating that the 3 µm OH band could possibly be due to the adsorbed terrestrial water or weathering. Choe et al. (2010) also reported the presence of altered chondrule mesostasis and phyllosilicate-rich matrix in QUE 99038, though they argued that it is a C2-ung instead of CM2 chondrite. We argue that the characteristic features such as the presence of abundant olivine and pyroxene, low TGA mass loss, and significantly ordered carbon structures (see below) are not consistent with either classification. In any case, the reason for the observed differences in different investigations is currently unclear. Brecciated samples often present different petrographic characteristics as they contain different lithologies; however, whether QUE 99038 is a brecciated meteorite or not is currently unknown.

Our Raman spectroscopic investigation shows that QUE 99038 contains polyaromatic organic matter whose structural properties are very similar to those of CV3 chondrites (Fig. 7). Having the narrowest D bandwidth, it is certainly a thermally metamorphosed chondrite. Spectral parameters of the second-order carbon bands can be used to discriminate between the CV3 subtypes (Yesiltas, Young, et al., 2021). Because QUE 99038 always plots within the CV3 chondrites in the figures presented above, its first- and second-order carbon peak parameters were compared with those of $CV3_{oxA}$, $CV3_{oxB}$, and $CV3_{red}$ chondrites to check whether it shows any similarities with any of the CV3 subtypes. Figure 11a and 11b present the comparison of first-order band parameters of CV3 subtypes. $CV3_{oxA}$ chondrites (green area) have higher I_D/I_G and lower Γ_D values than $CV3_{oxB}$ chondrites (blue area), and the width of the D band generally appears at higher wave numbers (with some overlap) than that of $CV3_{oxB}$ chondrites. $CV3_{red}$ chondrites exhibit large variations in their spectral parameters. One of the $CV3_{red}$ chondrites, MIL 07681, plots in close proximity to $CV3_{oxA}$ chondrites (Fig. 11a–c). We also include the same parameters of C2-ung chondrites in Fig. 11a and 11b for comparison. QUE 99038 (red star) plots significantly away from C2-ung chondrites and rather plots in close proximity to $CV3_{oxA}$ chondrites. C2-ung chondrites plot in upper regions of the graphs. Tagish Lake and Tarda have very similar parameters, and EET 83226 is intermediate. Furthermore, investigation of the second-order band parameters shows that the QUE 99038 has the highest I_{2D}/I_{D+G} ratios (~4), falling near $CV3_{oxA}$ chondrites (Fig. 11c), and plots quite higher than $CV3_{oxB}$ chondrites (~1). As such, QUE 99038 appears very similar to $CV3_{oxA}$ chondrites based on the Raman spectral parameters of its polyaromatic organic matter.

Is EET 83226 an Anomalous CO3 Chondrite?

Previous work showed that EET 83226 contains abundant small chondrules, mineral grains set in a moderate amount of dark brown to black opaque matrix, little Fe-Ni and sulfides, forsteritic olivine, and little pyroxene. Olivine in EET 83226 appears to be extensively zoned such that Fe/(Fe+Mg) ratio spans a wide range, and FeO abundance increases up to 45 wt

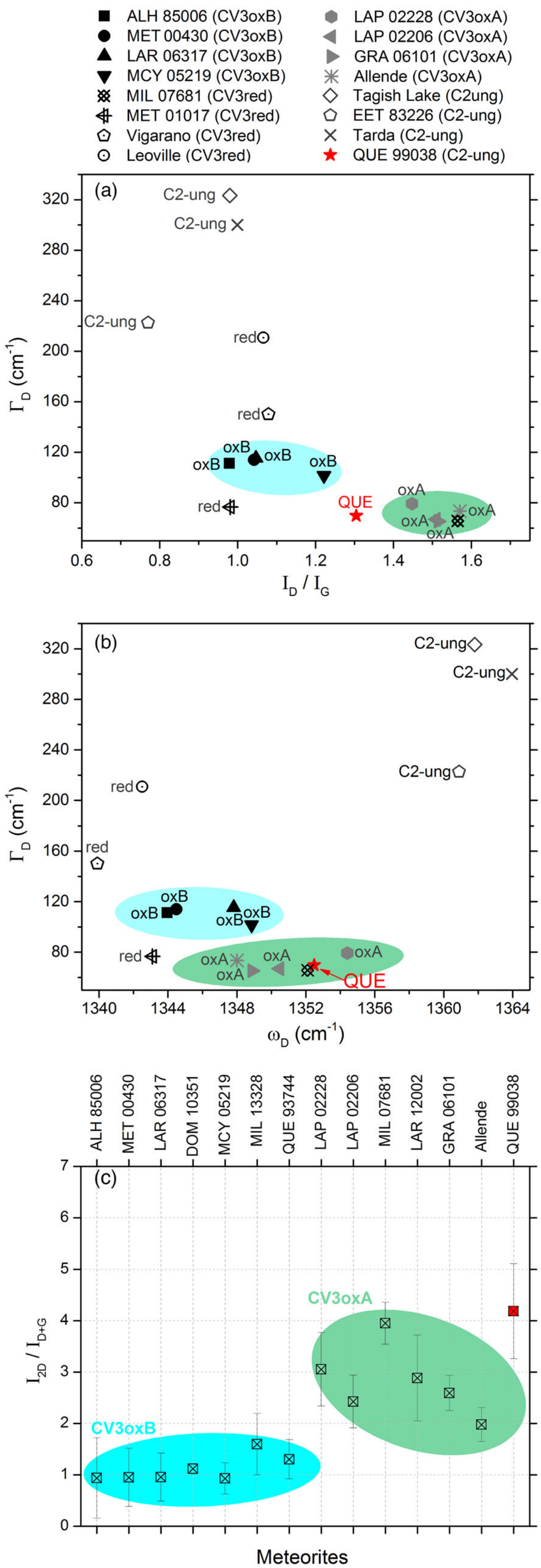

Fig. 11. Comparison of QUE 99038 with other C2-ung chondrites and CV3 subtypes based on the Raman spectroscopic data. CV3$_{oxA}$, CV3$_{oxB}$, and MIL 07681 data are from Yesiltas, Young, et al. (2021). CV3$_{red}$ (MET 01017, Vigarano, and Leoville) data are from Busemann et al. (2007).

% in the rims relative to the cores (Kloeck et al., 1989). Despite currently being classified as a C2-ung chondrite, EET 83226 presents similarities with the CV-CK clan, CM, and CO chondrites. It shows weak associations with the CV-CK clan and CO chondrites due to their somewhat similar bulk chemical compositions and mean chondrule diameters (Abreu et al., 2018); however, the bulk chemistry of EET 83226 is not clearly related to any of the known chondrite group. The 3 µm infrared hydration band of EET 83226 does not appear consistent with Tagish Lake (C2-ung) and rather resembles CM chondrites (Takir et al., 2019), although its oxygen isotopic composition is similar to CO chondrites and plots far from CM chondrites (Fig. 12). Abreu et al. (2018) suggested that EET 83226 should be reclassified as an anomalous CO chondrite. Our Raman spectroscopic investigation shows that EET 83226 plots far away from C2-ung chondrites and plots closer to CO3 chondrites. In this context, our results support the suggestion by Abreu et al. (2018).

FGRs are characteristic features of CM2 (Brearley, 2021; Hua et al., 2002; Huss et al., 2005; Lauretta et al., 2000; Metzler et al., 1992; Zega & Buseck, 2003; Zolensky et al., 1993) and some CO3 chondrites (Brearley, 1993; Brearley et al., 1995; Haenecour et al., 2018). The rims may have formed and accreted onto the chondrules in the solar nebula (Brearley, 1993; Chizmadia & Brearley, 2008; Ciesla et al., 2003; Hua et al., 1996; Metzler et al., 1992). Alternatively, Brearley and Geiger (1991), Tomeoka and Tanimura (2000), Sears et al. (1993), Trigo-Rodriguez et al. (2006) argued that the rims may have formed in the parent body through regolith processes such as alteration, metamorphism, compaction, and gardening. In the latter scenario, the rims are expected to be fragmented and discontinuous due to disruptive process in the parent body. As seen in Fig. 3, most chondrules in EET 83226 are surrounded by fragmented discontinuous rims, suggesting a parent body origin for the rims (i.e., in a regolith environment), rather than being nebula products, though more detailed examinations of many more rims are needed to determine their origin.

Is Tarda a Sample of D-Type Asteroids?

Tarda is the latest C2-ung chondrite as of today. It is an extremely friable carbonaceous chondrite with

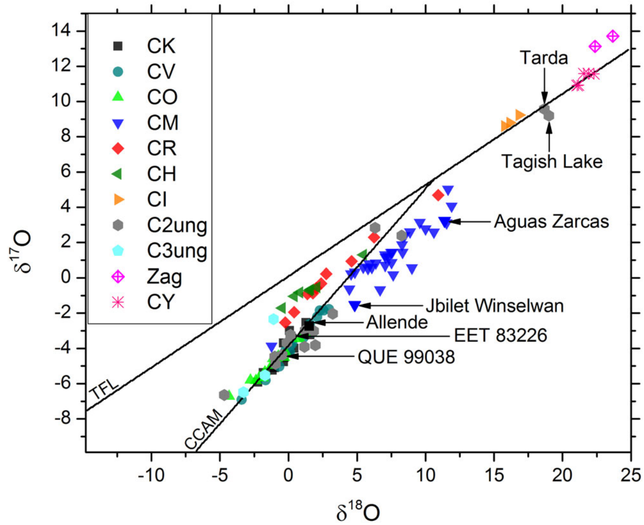

Fig. 12. Oxygen isotopic composition of various meteorite groups. TFL, terrestrial fractionation line. CCAM, carbonaceous chondrite anhydrous mineral line. Data for Tarda are from Meteoritical Bulletin 109 (Gattacceca et al., 2020); CM, CR, CI, CY, Allende, and C2-ung data are from Clayton and Mayeda (1999) and Tonui et al. (2014); CV and CK data are from Greenwood et al. (2010), CO data are from Greenwood and Franchi (2004), AZ data are from Meteoritical Bulletin 108 (Gattacceca et al., 2021), EET 83226 and C3-ung data are from Torrano et al. (2021), and Zag data are from Zolensky et al. (2003) and Kebukawa, Alexander, et al. (2019) and Kebukawa, Ito, et al. (2019).

matte black interior and dispersed ~1 mm diameter white grains. Chondrules are small and set in a dark matrix along with some forsterite. The fine-grained matrix is dominated by phyllosilicates, with lesser amounts of magnetite, carbonates, and troilite. Magnetite is found to be scattered throughout the sample in the form of framboids, platelets, and individual spherules. Oxygen isotopic composition of C2-ung chondrites spans a large range (Fig. 12), and Tarda plots very close to Tagish Lake, CI, and CY chondrites near the upper right part of the graph. Other C2-ung chondrites plot further down the graph and on the CCAM line, suggesting a diverse isotopic composition for the C2-ung chondrites (Fig. 12). In terms of oxygen isotopic composition, aqueous alteration, and thermal metamorphic history, Tarda looks very similar to Tagish Lake as suggested by Marrocchi et al. (2021), and consistent with being a C2-ung chondrite as it does not show similarities with members of other well-established groups. Carbonaceous chondrites are most likely samples of C-type asteroids, though Tagish Lake (Hiroi et al., 2001), WIS 91600 (Hiroi et al., 2005), and Tarda (Marrocchi et al., 2021) have been tentatively linked to D-type asteroids. Hiroi et al. (2022) recently argued that Tagish Lake is the only possible meteorite from D-type asteroids on the bases that visible near-infrared reflectance spectra of WIS 91600 and Tarda differ from those of D-type asteroids. This present study alone is unable to unambiguously establish this pairing. It would be interesting to conduct more detailed investigation to check this possibility as a future work. The Japan Aerospace Exploration Agency's (JAXA) Martian Moons eXploration (MMX) spacecraft will return samples from the Martian moon Phobos (Kuramoto et al., 2022). As Phobos could be a D-type asteroid, the MMX mission will be able to provide more definitive links between D-type asteroids and the meteorites in the collection.

Hydrated Versus Less Hydrated Meteorites

Some of the meteorites investigated in this work exhibit phyllosilicate-rich matrix and their infrared spectra present a broad band near 3400 cm^{-1} due to OH. However, some of them are more hydrated (contain more OH) than others. In this work, Tarda, Tagish Lake, Aguas Zarcas, and Jbilet Winselwan are considered hydrated carbonaceous chondrites. Tarda is very similar to Tagish Lake; they present very similar total mass loss upon heating, and present very similar thermal metamorphic histories deduced from the Raman spectral parameters of their respective organic matter. Jbilet Winselwan presents slightly less total mass loss between 200 and 900 °C upon heating, which indicates a relatively dehydrated matrix for Jbilet Winselwan, as previously indicated by Russell et al. (2014), Zolensky et al. (2016), and King et al. (2019). QUE 99038 and Allende are considered anhydrous. They both have similar near-infrared (NIR) spectra, presenting 1 and 2 μm bands, characteristic of anhydrous silicates (Gillis-Davis et al., 2017; Takir et al., 2013). Lack of such NIR features in EET 83226 indicates relatively aqueously altered composition.

The spectroscopic characteristics and degree of hydration of the Tarda meteorite are generally consistent with Tagish Lake. FT-IR spectra indicate abundant carbonates in Tarda and Tagish Lake. The TGA data are consistent with the FT-IR data, as Tarda and Tagish Lake exhibit the highest mass loss among the considered samples (Fig. 10). King, Bates, et al. (2021) and Garvie and Trif (2021) reported ~13 wt% TGA mass loss between 200 and 800 °C for Tarda, which is the same as ours, and thus, our TGA data are in good agreement with the reported TGA data for Tarda. Thus, the order of hydration obtained by TGA is as follows: CI1 (Orgueil) > Tarda ≈ Tagish Lake ≈ CR1(GRO 95577) ≥ CM2 (Aguas Zarcas and Murchison) > heated CM2 (Jbilet Winselwan and ALH 84033). Raman D and G band parameters of Tarda and Tagish Lake are consistent as well and indicate highly disordered carbon due to minimal thermal metamorphism. Unlike Tarda, QUE 99038 and EET 83226 are not very comparable to type 2 carbonaceous chondrites on the bases of their anhydrous mineralogy. They are rather similar to type 3 chondrites.

Comparison with Other Chondrite Groups

Bulk oxygen isotopic composition is one of the main criteria and often a useful indicator of meteorite classification, including carbonaceous chondrites, though some overlap between the groups does exist. Hewins et al. (2021) divided the ungrouped C2 chondrites into two clusters, C2-ung1 and C2-ung2, based on their oxygen isotope distributions. These clusters fall near the upper and lower end of the oxygen isotope distribution of CM chondrites, respectively. Oxygen isotopic compositions of the meteorites considered in our work are given in Fig. 12. Based on Hewins et al. (2021), QUE 99038 and EET 83226 fall within the C2-ung2 cluster; however, their oxygen isotopic compositions overlap with those of CV3 and CO chondrites as well and the C2-ung2 subclassification seems unhelpful for differentiation purposes in our case. Tarda falls within the C2-ung1 chondrite range along with Tagish Lake, and their similarity is well supported with oxygen isotopic compositions. Irving et al. (2022) recently presented evidence for a new chondrite group (CT) and reclassified several meteorites, including C2-ung and C3-ung chondrites, into the CT chondrite group. Comparison of the oxygen isotopic compositions suggest that none of the ungrouped chondrites studied in this work can be regarded as a CT chondrite either. Krämer Ruggiu et al. (2021) studied several ungrouped chondrites and divided them into six petrographic groups based on their texture, mineralogy, aqueous alteration, and thermal metamorphism histories. Chondrule size of QUE 99038 seems to match well with groups C and E (experienced moderate-to-significant thermal metamorphism).

Based on the smooth lithophile and siderophile/chalcophile patterns, Choe et al. (2010) suggested that the bulk composition of QUE 99038 may have been mostly inherited from the solar nebula. As its composition does not exactly resemble any of the well-established carbonaceous chondrite groups, the types of processes that can yield such a composition as in QUE 99038 are currently not fully known and clearly present a conundrum. Significant thermal metamorphism in the parent body could be argued as the reason for its bulk composition. In other words, the dehydrated nature of QUE 99038 could be due to short-term heating as seen in CY or heated CM-type carbonaceous chondrites (King et al., 2019). Nakamura (2005) and King, Schofield, et al. (2021) reported the characteristics of post-hydration thermal metamorphism in chondrites and provided properties of metamorphic stages I through IV. QUE 99038 might be a significantly heated CM chondrite, perhaps stage IV (>750 °C). However, the heated and unheated CM chondrites typically show similar Raman spectral characteristics, as in the case of Jbilet Winselwan (stage II, 300–500 °C) (Fig. 7) and Y-86720 (stage IV) (Busemann et al., 2007). Therefore, QUE 99038 is clearly distinguished from the heated CM and CY chondrites.

Comparison with Xenolithic Clasts

The C2-ung chondrites studied here (QUE 99038, EET 83226, and Tarda) are somewhat similar to the members of known carbonaceous chondrite groups but not without differences. They show petrological and compositional variations among each other that are larger than the variations seen within each group of well-established chondrites. Such variations and characteristics are also seen in xenolithic clasts found in various meteorites. For example, the xenolithic clasts in the Zag meteorite (H5) are similar to Tagish Lake (Kebukawa et al., 2020; Kebukawa, Ito, et al., 2019), and heavily metamorphosed clasts found in Mokoia and Yamato-86009 (CV) (Jogo et al., 2013). The $\delta^{17}O$ and $\delta^{18}O$ values of the Zag clasts plot close to those of Tarda and Tagish Lake (Kebukawa, Ito, et al., 2019; Zolensky et al., 2003) (Fig. 12). The IR spectrum of the Zag clast presents features characteristic of a highly carbonate-rich composition, similar to Tarda and Tagish Lake, which is comparable to typical CI, CM, and CR chondrites (Kebukawa et al., 2020).

Similar to Tarda and Tagish Lake, the Zag clast is also linked to D-type asteroids (Kebukawa et al., 2020; Kebukawa, Ito, et al., 2019). Such volatile-rich fragile materials are expected to survive better as xenolithic clasts than as meteorites. One reason is that meteorites are subjected to harsh conditions when they enter the Earth's atmosphere, while xenolithic clasts are incorporated into their host meteorite parent bodies through rather low-velocity impacts and are protected in their host meteorites. This might in fact be the case as only one clast is associated with a D-type asteroid, but many more clasts are associated with C-type asteroids (parent bodies of other carbonaceous chondrites). The majority of xenolithic clasts also appear similar to CI, CM, or CR chondrites (and a few to CV chondrites) in terms of their mineralogy (Zolensky et al., 1996), bulk oxygen isotopes (Clayton & Mayeda, 1999), and carbonaceous matter (Visser et al., 2018). This is somewhat consistent and correlated with the population of D-type asteroids around the

Main Belt (~2 to 3 AU), which is roughly two orders of magnitude lower than C-type asteroid population within the same region (DeMeo & Carry, 2014).

CONCLUSIONS

Type 2 ungrouped carbonaceous chondrites represent a very small fraction of all known carbonaceous chondrites. They are not easily classified into one of the well-established groups due to compositional and petrological differences and anomalies. They can potentially represent different aspects of asteroids and their regolith material. In this work, we focused on three C2-ung chondrites, QUE 99038, EET 83226, and Tarda, and investigated their chemical composition, macromolecular carbon content, and hydration state. QUE 99038 contains anhydrous mineralogy. It clearly experienced moderate-to-significant thermal metamorphism, evident from its petrographic properties and textures as well as the presence of anhydrous silicates. It does not look like CM chondrites (heated or otherwise), its polyaromatic organic structures and their Raman spectral parameters perfectly resemble A-type oxidized CV3 chondrites. Oxygen isotopic composition of QUE 99038 overlaps well with CV and CO chondrites, though its petrology and chemistry are different from CO chondrites. EET 83226 is a highly porous chondrite with a clastic texture and mainly anhydrous mineralogy. It consists of numerous large chondrules enclosed with FGRs, which are often observed in CM2 and CO3 chondrites. The FGRs are mostly fragmented and discontinuous, suggesting a formation mechanism in a regolith environment through disruptive parent body processes. Its oxygen isotopic composition plots in the vicinity of CO, CV, and CK chondrites. Raman spectral parameters of organic matter in EET 83226 plot far away from C2-ung chondrites, but rather close to CO3 chondrites. Tarda does not show similarities with members of other well-established groups. Unlike QUE 99038 and EET 83226, Tarda is consistent with being a C2-ung chondrite and is very similar to Tagish Lake in many ways. Tarda and Tagish Lake present very similar TGA mass loss upon heating, and present very similar thermal metamorphic histories deduced from the Raman spectral parameters of their respective organic matter. Overall, despite their current classifications, QUE 99038 and EET 83226 are not quite compatible with type 2 carbonaceous chondrites. They are rather similar to type 3 chondrites. Our Raman spectral data suggest CV and CO classifications, respectively. The kind of processes that can result in such chemical compositions as in QUE 99038 and EET 83226 are currently not fully known and, in this context, clearly present a conundrum.

Acknowledgments—We are grateful to reviewers A. King, M. Komatsu, and M. Matsuoka for thoughtful and constructive reviews that markedly improved the manuscript. We thank the Meteorite Working Group at the NASA Johnson Space Center for providing the QUE 99038 and EET 83226 meteorite samples. We also thank M. A. Oral for assistance with sample preparation, and Sinem Leventer for assistance with the electron microscope. This work was supported by TUBITAK (PI: M. Yesiltas, projects #119 N207 and #120Y115) and RISE2 node of NASA-SSERVI (PI: T. D. Glotch).

Data Availability Statement—Data available on request from the authors.

Editorial Handling—Dr. Akira Yamaguchi

REFERENCES

Abreu, N. M., Louro, M. D., Friedrich, J. M., Schrader, D. L., and Greenwood, R. C. 2018. Elephant Moraine (EET) 83226: A Clastic, Type 2 Carbonaceous Chondrite with Affinities to the CO Chondrites (Abstract #2083). 49th Lunar and Planetary Science Conference. CD-ROM.

Bates, H. C., Donaldson Hanna, K. L., King, A. J., Bowles, N. E., and Russell, S. S. 2021. A Spectral Investigation of Aqueously and Thermally Altered CM, CM-an, and CY Chondrites under Simulated Asteroid Conditions for Comparison with OSIRIS-REx and Hayabusa2 Observations. *Journal of Geophysical Research: Planets* 126: e2021JE006827. https://doi.org/10.1029/2021JE006827.

Bates, H. C., King, A. J., Donaldson Hanna, K. L., Bowles, N. E., and Russell, S. S. 2020. Linking Mineralogy and Spectroscopy of Highly Aqueously Altered CM and CI Carbonaceous Chondrites in Preparation for Primitive Asteroid Sample Return. *Meteoritics & Planetary Science* 55: 77–101.

Beyssac, O., Goffé, B., Petitet, J. P., Froigneux, E., Moreau, M., and Rouzaud, J. N. 2003. On the Characterization of Disordered and Heterogeneous Carbonaceous Materials by Raman Spectroscopy. *Spectrochimica Acta Part A: Molecular and Biomolecular Spectroscopy* 59: 2267–76.

Beyssac, O., Rouzaud, J. N., Goffe, B., Brunet, F., and Chopin, C. 2002. Graphitization in a High-Pressure, Low-Temperature Metamorphic Gradient: A Raman Microspectroscopy and HRTEM Study. *Contributions to Mineralogy and Petrology* 143: 19–31.

Bland, P. A., Alard, O., Benedix, G. K., Kearsley, A. T., Menzies, O. N., Watt, L. E., and Rogers, N. W. 2005. Volatile Fractionation in the Early Solar System and Chondrule/Matrix Complementarity. *Proceedings of the National Academy of Sciences* 102: 13755–60.

Bottom, R. 2008. Thermogravimetric Analysis. In *Principles and Applications of Thermal Analysis*, edited by P. Gabbott, 87–118. Oxford: Blackwell Publishing Ltd.

Brearley, A. J. 1993. Matrix and Fine-Grained Rims in the Unequilibrated CO3 Chondrite, ALHA77307: Origins and Evidence for Diverse, Primitive Nebular Dust

Components. *Geochimica et Cosmochimica Acta* 57: 1521–50.
Brearley, A. J. 2006. The Action of Water. In *Meteorites and the Early Solar System II*, edited by D. S. Lauretta and H. Y. McSween, 587–624. Tucson, Arizona: University of Arizona Press.
Brearley, A. J. 2021. Nanophase Iron Carbides in Fine-Grained Rims in CM2 Carbonaceous Chondrites: Formation of Organic Material by Fischer–Tropsch Catalysis in the Solar Nebula. *Meteoritics & Planetary Science* 56: 108–26.
Brearley, A. J., Bajt, S., and Sutton, S. R. 1995. Distribution of Moderately Volatile Trace Elements in Fine-Grained Chondrule Rims in the Unequilibrated CO3 Chondrite, ALH A77307. *Geochimica et Cosmochimica Acta* 59: 4307–16.
Brearley, A. J., and Geiger, T. 1991. Mineralogical and Chemical Studies Bearing on the Origin of Accretionary Rims in the Murchison CM2 Carbonaceous Chondrite (Abstract). *Meteoritics* 26: 323.
Brown, P. G., Hildebrand, A. R., Zolensky, M. E., Grady, M., Clayton, R. N., Mayeda, T. K., Tagliaferri, E., et al. 2000. The Fall, Recovery, Orbit, and Composition of the Tagish Lake Meteorite: A New Type of Carbonaceous Chondrite. *Science* 290: 320–5.
Busemann, H., Alexander, M. O'D., and Nittler, L. R. 2007. Characterization of Insoluble Organic Matter in Primitive Meteorites by microRaman Spectroscopy. *Meteoritics & Planetary Science* 42: 1387–416.
Casiraghi, C. F. A. R. J., Ferrari, A. C., and Robertson, J. 2005. Raman Spectroscopy of Hydrogenated Amorphous Carbons. *Physical Review B* 72: 085401.
Che, C., and Glotch, T. D. 2012. The Effect of High Temperatures on the Mid-to-Far-Infrared Emission and Near-Infrared Reflectance Spectra of Phyllosilicates and Natural Zeolites: Implications for Martian Exploration. *Icarus* 218: 585–601.
Che, C., Glotch, T. D., Bish, D. L., Michalski, J. R., and Xu, W. 2011. Spectroscopic Study of the Dehydration and/or Dehydroxylation of Phyllosilicate and Zeolite Minerals. *Journal of Geophysical Research: Planets* 116: E5. https://doi.org/10.1029/2010JE003740.
Chennaoui Aoudjehane, H., Agee, C. B., Ziegler, K., Garvie, L. A. J., Irving, A., Sheikh, D., Carpenter, P. K., Zolensky, M., Schmitt-Kopplin, P., and Trif, L. 2021. Tarda (C2-Ung): A New and Unusual Carbonaceous Chondrite Meteorite Fall from Morocco (Abstract #1928). 52nd Lunar and Planetary Science Conference. CD-ROM.
Chizmadia, L. J., and Brearley, A. J. 2008. Mineralogy, Aqueous Alteration, and Primitive Textural Characteristics of Fine-Grained Rims in the Y-791198 CM2 Carbonaceous Chondrite: TEM Observations and Comparison to ALHA81002. *Geochimica et Cosmochimica Acta* 72: 602–25.
Choe, W. H., Huber, H., Rubin, A. E., Kallemeyn, G. W., and Wasson, J. T. 2010. Compositions and Taxonomy of 15 Unusual Carbonaceous Chondrites. *Meteoritics & Planetary Science* 45: 531–54.
Ciesla, F. J., Lauretta, D. S., Cohen, B. A., and Hood, L. L. 2003. A Nebular Origin for Chondritic Fine-Grained Phyllosilicates. *Science* 299: 549–52.
Clayton, R. N., and Mayeda, T. K. 1999. Oxygen Isotope Studies of Carbonaceous Chondrites. *Geochimica et Cosmochimica Acta* 63: 2089–104.
Cloutis, E. A., Hudon, P., Hiroi, T., and Gaffey, M. J. 2012. Spectral Reflectance Properties of Carbonaceous Chondrites 4: Aqueously Altered and Thermally Metamorphosed Meteorites. *Icarus* 220: 586–617.
DeMeo, F. E., and Carry, B. 2014. Solar System Evolution from Compositional Mapping of the Asteroid Belt. *Nature* 505: 629–34.
Dubinin, M. M. 1980. Water Vapor Adsorption and the Microporous Structures of Carbonaceous Adsorbents. *Carbon* 18: 355–64.
Ferrari, A. C., and Robertson, J. 2000. Interpretation of Raman Spectra of Disordered and Amorphous Carbon. *Physical Review B* 61: 14095–107.
Garenne, A., Beck, P., Montes-Hernandez, G., Chiriac, R., Toche, F., Quirico, E., Bonal, L., and Schmitt, B. 2014. The Abundance and Stability of "Water" in Type 1 and 2 Carbonaceous Chondrites (CI, CM and CR). *Geochimica et Cosmochimica Acta* 137: 93–112.
Garvie, L. A. J., and Trif, L. 2021. Bulk Mineralogy of the Tarda (C2-Ung) 2020 Fall: Results from Powder XRD and Thermal (TG-DSC-MSEGA) Analysis (Abstract #2548). 52nd Lunar and Planetary Science Conference. CD-ROM.
Gattacceca, J., McCubbin, F. M., Bouvier, A., and Grossman, J. N. 2020. The Meteoritical Bulletin, No. 108. *Meteoritics & Planetary Science* 55: 1146–50.
Gattacceca, J., McCubbin, F. M., Grossman, J., Bouvier, A., Bullock, E., Chennaoui Aoudjehane, H., Debaille, V., et al. 2021. The Meteoritical Bulletin, No. 109. *Meteoritics & Planetary Science* 56: 1626–30.
Gillis-Davis, J. J., Lucey, P. G., Bradley, J. P., Ishii, H. A., Kaluna, H. M., Misra, A., and Connolly, H. C., Jr. 2017. Incremental Laser Space Weathering of Allende Reveals Non-lunar like Space Weathering Effects. *Icarus* 286: 1–14.
Gilmour, C. M., Herd, C. D., and Beck, P. 2019. Water Abundance in the Tagish Lake Meteorite from TGA and IR Spectroscopy: Evaluation of Aqueous Alteration. *Meteoritics & Planetary Science* 54: 1951–72.
Grady, M. M. 2000. *Catalogue of Meteorites*, 5th ed. New York: Cambridge University Press.
Greenwood, R. C., and Franchi, I. A. 2004. Alteration and Metamorphism of CO3 Chondrites: Evidence from Oxygen and Carbon Isotopes. *Meteoritics & Planetary Science* 39: 1823–38.
Greenwood, R. C., Franchi, I. A., Kearsley, A. T., and Alard, O. 2010. The Relationship between CK and CV Chondrites. *Geochimica et Cosmochimica Acta* 74: 1684–705.
Greshake, A., Krot, A. N., Meibom, A., Weisberg, M. K., Zolensky, M. E., and Keil, K. 2002. Heavily-Hydrated Lithic Clasts in CH Chondrites and the Related, Metal-Rich Chondrites Queen Alexandra Range 94411 and Hammadah al Hamra 237. *Meteoritics & Planetary Science* 37: 281–93.
Grossman, J. N., and Zipfel, J. 2001. The Meteoritical Bulletin, No. 85. *Meteoritics & Planetary Science* 36: A293–322.
Haenecour, P., Floss, C., Zega, T. J., Croat, T. K., Wang, A., Jolliff, B. L., and Carpenter, P. 2018. Presolar Silicates in the Matrix and Fine-Grained Rims around Chondrules in Primitive CO3. 0 Chondrites: Evidence for Pre-Accretionary Aqueous Alteration of the Rims in the Solar Nebula. *Geochimica et Cosmochimica Acta* 221: 379–405.

Hewins, R. H., Zanetta, P. M., Zanda, B., Le Guillou, C., Gattacceca, J., Sognzoni, C., Pont, S., Piani, L., Rigaudier, T., Leroux, H., and Brunetto, R. 2021. NORTHWEST AFRICA (NWA) 12563 and Ungrouped C2 Chondrites: Alteration Styles and Relationships to Asteroids. *Geochimica et Cosmochimica Acta* 311: 238–73.

Hiroi, T., Ohtsuka, K., Zolensky, M. E., Rutherford, M. J., and Milliken, R. E. 2022. Tagish Lake is Still the Only Possible Meteorite Sample from D-Type Asteroids (Abstract #1149). 53rd Lunar and Planetary Science Conference. CD-ROM.

Hiroi, T., Tonui, E., Pieters, C.M., Zolensky, M.E., Ueda, Y., Miyamoto, M., and Sasaki, S. 2005. Meteorite WIS91600: A New Sample Related to a D-or T-Type Asteroid (Abstract #1564). 36th Lunar and Planetary Science Conference. CD-ROM.

Hiroi, T., Zolensky, M. E., and Pieters, C. M. 2001. The Tagish Lake Meteorite: A Possible Sample from a D-Type Asteroid. *Science* 293: 2234–6.

Hua, X., Wang, J., and Buseck, P. R. 2002. Fine-Grained Rims in the Allan Hills 81002 and Lewis Cliff 90500 CM2 Meteorites: Their Origin and Modification. *Meteoritics & Planetary Science* 37: 229–44.

Hua, X., Zinner, E. K., and Buseck, P. R. 1996. Petrography and Chemistry of Fine-Grained Dark Rims in the Mokoia CV3 Chondrite: Evidence for an Accretionary Origin. *Geochimica et Cosmochimica Acta* 60: 4265–74.

Huber, H., Rubin, A. E., and Wasson, J. T. 2006. Bulk Compositions and Petrographic Characteristics of Ten Unusual Carbonaceous Chondrites (Abstract #2381). 37th Lunar and Planetary Science Conference. CD-ROM.

Huss G. R., Alexander C. M.O'D. Palme H., Bland P. A., and Wasson J. T. 2005. Genetic Relationships Between Chondrules, Fine-Grained Rims, and Interchondrule Matrix. In *Chondrites and the Protoplanetary Disk*, edited by A. N. Krot, E. R. D. Scott, and B. Reipurth. ASP Conference Series, vol. 341, 701–31. San Francisco: Astronomical Society of the Pacific.

Huss, G. R., Rubin, A. E., and Grossman, J. N. 2006. Thermal Metamorphism in Chondrites. In *Meteorites and the Early Solar System II*, edited by D. S. Lauretta and H. Y. McSween, 567–86. Tucson, Arizona: University of Arizona Press.

Irving, A. J., Gattacceca, J., Ziegler, K., Sonzogni, C., Carpenter, P. K., and Garvie, L. A. J. 2022. CT Chondrites: A Newly Recognized Carbonaceous Chondrite Group with Multiple Members, Including Telakoast 001, Chwichiya 002, and Cimarron (Abstract #2046). 53rd Lunar and Planetary Science Conference. CD-ROM.

Jochum, K. P., Willbold, M., Raczek, I., Stoll, B., and Herwig, K. 2005. Chemical Characterisation of the USGS Reference Glasses GSA-1G, GSC-1G, GSD-1G, GSE-1G, BCR-2G, BHVO-2G and BIR-1G Using EPMA, ID-TIMS, ID-ICP-MS and LA-ICP-MS. *Geostandards and Geoanalytical Research* 29: 285–302.

Jogo, A. K., Krot, A. N., and Nagashima, K. 2013. Metamorphosed Clasts in the CV Carbonaceous Chondrite Breccias Mokoia and Yamato 86009: Evidence for Strong Thermal Metamorphism on the CV Parent Asteroid. In *International Astrobiology Workshop, 2013*, 21–2. Houston, TX: LPI Contribution No. 1766, Lunar and Planetary Institute.

Kallemeyn, G. W., and Wasson, J. T. 1981. The Compositional Classification of Chondrites—I. The Carbonaceous Chondrite Groups. *Geochimica et Cosmochimica Acta* 45: 1217–30.

Kebukawa, Y., Alexander, C. M. O'D., and Cody, G. D. 2019. Comparison of FT-IR Spectra of Bulk and Acid Insoluble Organic Matter in Chondritic Meteorites: An Implication for Missing Carbon during Demineralization. *Meteoritics & Planetary Science* 54: 1632–41.

Kebukawa, Y., Ito, M., Zolensky, M. E., Greenwood, R. C., Rahman, Z., Suga, H., Nakato, A., et al. 2019. A Novel Organic-Rich Meteoritic Clast from the Outer Solar System. *Scientific Reports* 9: 1–8.

Kebukawa, Y., Zolensky, M. E., Ito, M., Ogawa, N. O., Takano, Y., Ohkouchi, N., Nakato, A., et al. 2020. Primordial Organic Matter in the Xenolithic Clast in the Zag H Chondrite: Possible Relation to D/P Asteroids. *Geochimica et Cosmochimica Acta* 271: 61–77.

Kerraouch, I., Bischoff, A., Zolensky, M. E., Pack, A., Patzek, M., Hanna, R. D., Fries, M. D., et al. 2021. The Polymict Carbonaceous Breccia Aguas Zarcas: A Potential Analog to Samples Being Returned by the OSIRIS-REx and Hayabusa2 Missions. *Meteoritics & Planetary Science* 56: 277–310.

King, A. J., Bates, H. C., Krietsch, D., Busemann, H., Clay, P. L., Schofield, P. F., and Russell, S. S. 2019. The Yamato-Type (CY) Carbonaceous Chondrite Group: Analogues for the Surface of Asteroid Ryugu? *Geochemistry* 79: 125531.

King, A. J., Bates, H. C., Schofield, P. F., and Russell, S. S. 2021. The Bulk Mineralogy and Water Contents of the Carbonaceous Chondrite Falls Kolang and Tarda (Abstract #2548). 52nd Lunar and Planetary Science Conference. CD-ROM.

King, A. J., Schofield, P. F., and Russell, S. S. 2021. Thermal Alteration of CM Carbonaceous Chondrites: Mineralogical Changes and Metamorphic Temperatures. *Geochimica et Cosmochimica Acta* 298: 167–90.

King, A. J., Solomon, J. R., Schofield, P. F., and Russell, S. S. 2015. Characterising the CI and CI-Like Carbonaceous Chondrites Using Thermogravimetric Analysis and Infrared Spectroscopy. *Earth, Planets and Space* 67: 1–12.

Kloeck, W., Thomas, K. L., and McKay, D. S. 1989. Identification of Solar Nebula Condensates in Interplanetary Dust Particles, Unequilibrated Ordinary Chondrites and Carbonaceous Chondrites (Abstract #522). 20th Lunar and Planetary Science Conference. CD-ROM.

Kong, P., and Palme, H. 1999. Compositional and Genetic Relationship between Chondrules, Chondrule Rims, Metal, and Matrix in the Renazzo Chondrite. *Geochimica et Cosmochimica Acta* 63: 3673–82.

Krämer Ruggiu, L., Beck, P., Gattacceca, J., and Eschrig, J. 2021. Visible-Infrared Spectroscopy of Ungrouped and Rare Meteorites Brings Further Constraints on Meteorite-Asteroid Connections. *Icarus* 362: 114393.

Kuramoto, K., Kawakatsu, Y., Fujimoto, M., Araya, A., Barucci, M. A., Genda, H., Hirata, N., et al. 2022. Martian Moons Exploration MMX: Sample Return Mission to Phobos Elucidating Formation Processes of Habitable Planets. *Earth, Planets and Space* 74: 1–31.

Lauretta, D. S., Hua, X., and Buseck, P. R. 2000. Mineralogy of Fine-Grained Rims in the ALH 81002 CM Chondrite. *Geochimica et Cosmochimica Acta* 64: 3263–73.

Liu, Y., Hu, Z. C., Gao, S., Gunther, D., Xu, J., Gao, C. G., and Chen, H. H. 2008. In Situ Analysis of Major and Trace Elements of Anhydrous Minerals by LA-ICP-MS

without Applying an Internal Standard. *Chemical Geology* 257: 34–43.
MacPherson, G. 1985. *Antarctic Meteorite Newsletter* 8: 5. https://curator.jsc.nasa.gov/antmet/amn/previous_newsletters/antartic_meterorite_newsletter_vol_8_number_1.pdf
Marrocchi, Y., Avice, G., and Barrat, J. A. 2021. The Tarda Meteorite: A Window into the Formation of D-Type Asteroids. *The Astrophysical Journal Letters* 913: L9.
McBride, K., McCoy, T., and Welzenbach, L. 2001. QUE 99038. *Antarctic Meteorite Newsletters* 24: 12.
McDonough, W. F., and Sun, S. S. 1995. The Composition of the Earth. *Chemical Geology* 120: 223–53.
Meteoritical Bulletin Database. 2022. Accessed May 1, 2022. https://www.lpi.usra.edu/meteor/metbull.php.
Metzler, K., Bischoff, A., and Stöffler, D. 1992. Accretionary Dust Mantles in CM Chondrites: Evidence for Solar Nebula Processes. *Geochimica et Cosmochimica Acta* 56: 2873–97.
Miyamoto, M., and Zolensky, M. E. 1994. Infrared Diffuse Reflectance Spectra of Carbonaceous Chondrites: Amount of Hydrous Minerals. *Meteoritics* 29: 849–53.
Morlok, A., Schiller, B., Weber, I., Daswani, M. M., Stojic, A. N., Reitze, M. P., Gramse, T., et al. 2020. Mid-Infrared Reflectance Spectroscopy of Carbonaceous Chondrites and Calcium–Aluminum-Rich Inclusions. *Planetary and Space Science* 193: 105078.
Nakamura, T. 2005. Post-Hydration Thermal Metamorphism of Carbonaceous Chondrites. *Journal of Mineralogical and Petrological Sciences* 100: 260–72.
Nakamura-Messenger, K., Messenger, S., Keller, L. P., Clemett, S. J., and Zolensky, M. E. 2006. Organic Globules in the Tagish Lake Meteorite: Remnants of the Protosolar Disk. *Science* 314: 1439–42.
Pearce, N. J., Perkins, W. T., Westgate, J. A., Gorton, M. P., Jackson, S. E., Neal, C. R., and Chenery, S. P. 1997. A Compilation of New and Published Major and Trace Element Data for NIST SRM 610 and NIST SRM 612 Glass Reference Materials. *Geostandards Newsletter* 21: 115–44.
Potin, S., Beck, P., Bonal, L., Schmitt, B., Garenne, A., Moynier, F., Agranier, A., Schmitt-Kopplin, P., Malik, A. K., and Quirico, E. 2020. Mineralogy, Chemistry, and Composition of Organic Compounds in the Fresh Carbonaceous Chondrite Mukundpura: CM1 or CM2? *Meteoritics & Planetary Science* 55: 1681–96.
Rubin, A. E., and Wasson, J. T. 1987. Chondrules, Matrix and Coarse-Grained Chondrule Rims in the Allende Meteorite: Origin, Interrelationships and Possible Precursor Components. *Geochimica et Cosmochimica Acta* 51: 1923–37.
Rubin, A. E., and Wasson, J. T. 1988. Chondrules and Matrix in the Ornans CO3 Meteorite: Possible Precursor Components. *Geochimica et Cosmochimica Acta* 52: 425–32.
Russell, S. S., King, A. J., Schofield, P. F., Verchovsky, A. B., Abernethy, F., and Grady, M. M. 2014. The Jbilet Winselwan Carbonaceous Chondrite 1. Mineralogy and Petrology: Strengthening the Link between CM and CO Meteorites? (Abstract #5253). *Meteoritics & Planetary Science* 49: 345.
Ruzicka, A., Grossman, J., Bouvier, A., Herd, C. D. K., and Agee, C. B. 2015. The Meteoritical Bulletin, No. 101. *Meteoritics & Planetary Science* 50: 1661. https://doi.org/10.1111/maps.12490.
Sears, D. W., Benoit, P. H., and Jie, L. 1993. Two Chondrule Groups Each with Distinctive Rims in Murchison Recognized by Cathodoluminescence. *Meteoritics* 28: 669–75.
Sears, D. W. G., and Dodd, R. T. 1988. Overview and Classification of Meteorites. In *Meteorites and the Early Solar System*, edited by J. F. Kerridge and M. S. Matthews, 3–31. Tucson, Arizona: The University of Arizona Press.
Takir, D., Emery, J. P., Mcsween, H. Y., Jr., Hibbitts, C. A., Clark, R. N., Pearson, N., and Wang, A. 2013. Nature and Degree of Aqueous Alteration in CM and CI Carbonaceous Chondrites. *Meteoritics & Planetary Science* 48: 1618–37.
Takir, D., Stockstill-Cahill, K. R., Hibbitts, C. A., and Nakauchi, Y. 2019. 3-μm Reflectance Spectroscopy of Carbonaceous Chondrites Under Asteroid-Like Conditions. *Icarus* 333: 243–51.
Tomeoka, K., and Tanimura, I. 2000. Phyllosilicate-Rich Chondrule Rims in the Vigarano CV3 Chondrite: Evidence for Parent-Body Processes. *Geochimica et Cosmochimica Acta* 64: 1971–88.
Tonui, E., Zolensky, M., Hiroi, T., Nakamura, T., Lipschutz, M. E., Wang, M. S., and Okudaira, K. 2014. Petrographic, Chemical and Spectroscopic Evidence for Thermal Metamorphism in Carbonaceous Chondrites I: CI and CM Chondrites. *Geochimica et Cosmochimica Acta* 126: 284–306.
Torrano, Z. A., Schrader, D. L., Davidson, J., Greenwood, R. C., Dunlap, D. R., and Wadhwa, M. 2021. The Relationship Between CM and CO Chondrites: Insights from Combined Analyses of Titanium, Chromium, and Oxygen Isotopes in CM, CO, and Ungrouped Chondrites. *Geochimica et Cosmochimica Acta* 301: 70–90.
Trigo-Rodriguez, J. M., Rubin, A. E., and Wasson, J. T. 2006. Non-Nebular Origin of Dark Mantles around Chondrules and Inclusions in CM Chondrites. *Geochimica et Cosmochimica Acta* 70: 1271–90.
Visser, R., John, T., Menneken, M., Patzek, M., and Bischoff, A. 2018. Temperature Constraints by Raman Spectroscopy of Organic Matter in Volatile-Rich Clasts and Carbonaceous Chondrites. *Geochimica et Cosmochimica Acta* 241: 38–55.
Weisberg, M. K., McCoy, T. J., and Krot, A. N. 2006. Systematics and Evaluation of Meteorite Classification. In *Meteorites and the Early Solar System II*, edited by D. S. Lauretta and H. Y. McSween, Jr., 19–52. Tucson, Arizona: University of Arizona Press.
Yesiltas, M., Glotch, T. D., Jaret, S., Verchovsky, A. B., and Greenwood, R. C. 2019. Carbonaceous Matter in the Sariçiçek Meteorite. *Meteoritics & Planetary Science* 54: 1495–511.
Yesiltas, M., Glotch, T. D., and Kaya, M. 2021. Nanoscale Infrared Characterization of Dark Clasts and Fine-Grained Rims in CM2 Chondrites: Aguas Zarcas and Jbilet Winselwan. *ACS Earth and Space Chemistry* 5: 3281–96.
Yesiltas, M., Glotch, T. D., and Sava, B. 2021. Nano-FTIR Spectroscopic Identification of Prebiotic Carbonyl Compounds in Dominion Range 08006 Carbonaceous Chondrite. *Scientific Reports* 11: 1–9.
Yesiltas, M., Jaret, S., Young, J., Wright, S. P., and Glotch, T. D. 2018. Three-Dimensional Raman Tomographic Microspectroscopy: A Novel Imaging Technique. *Earth and Space Science* 5: 380–92.

Yesiltas, M., Kaya, M., Glotch, T. D., Brunetto, R., Maturilli, A., Helbert, J., and Ozel, M. E. 2020. Biconical Reflectance, Micro-Raman, and Nano-FTIR Spectroscopy of the Didim (H3-5) Meteorite: Chemical Content and Molecular Variations. *Meteoritics & Planetary Science* 55: 2404–21.

Yesiltas, M., and Kebukawa, Y. 2016. Associations of Organic Matter with Minerals in Tagish Lake Meteorite via High Spatial Resolution Synchrotron-Based FTIR Microspectroscopy. *Meteoritics & Planetary Science* 51: 584–95.

Yesiltas, M., Sedlmair, J., Peale, R. E., and Hirschmugl, C. J. 2017. Synchrotron-Based Three-Dimensional Fourier-Transform Infrared Spectro-Microtomography of Murchison Meteorite Grain. *Applied Spectroscopy* 71: 1198–208.

Yesiltas, M., Young, J., and Glotch, T. D. 2021. Thermal Metamorphic History of Antarctic CV3 and CO3 Chondrites Inferred from the First-and Second-Order Raman Peaks of Polyaromatic Organic Carbon. *American Mineralogist: Journal of Earth and Planetary Materials* 106: 506–17.

Zega, T. J., and Buseck, P. R. 2003. Fine-Grained-Rim Mineralogy of the Cold Bokkeveld CM Chondrite. *Geochimica et Cosmochimica Acta* 67: 1711–21.

Zolensky, M., Barrett, R., and Browning, L. 1993. Mineralogy and Composition of Matrix and Chondrule Rims in Carbonaceous Chondrites. *Geochimica et Cosmochimica Acta* 57: 3123–48.

Zolensky, M., Mikouchi, T., Hagiya, K., Ohsumi, K., Komatsu, M., Chan, Q. H., Le, L., Kring, D., Cato, M., Fagan, A. L., and Gross, J. 2016. Unique View of C Asteriod Regolith from the Jbilet Winselwan CM Chondrite (Abstract #2148). 47th Lunar and Planetary Science Conference. CD-ROM.

Zolensky, M. E., Clayton, R. N., Mayeda, T., Chokai, J., and Norton, O. R. 2003. Carbonaceous Chondrite Clasts in the Halite-Bearing H5 Chondrite Zag (Abstract #5216). *Meteoritics & Planetary Science Supplement* 38: A114.

Zolensky, M. E., Nakamura, K., Gounelle, M., Mikouchi, T., Kasama, T., Tachikawa, O., and Tonui, E. 2002. Mineralogy of Tagish Lake: An Ungrouped Type 2 Carbonaceous Chondrite. *Meteoritics & Planetary Science* 37: 737–61.

Zolensky, M. E., Weisberg, M. K., Buchanan, P. C., and Mittlefehldt, D. W. 1996. Mineralogy of Carbonaceous Chondrite Clasts in HED Achondrites and the Moon. *Meteoritics & Planetary Science* 31: 518–37.

SUPPORTING INFORMATION

Additional supporting information may be found in the online version of this article.

Table S1. Major (wt%) and trace element (ppm) composition of QUE 99038, EET 83226, and Tarda matrices.

Table S2. Raman spectral parameters of the first-order carbon bands observed in this work.

Fig. S1. Raman spectra of QUE 99038 (C2-ung) and Allende (CV3). The Raman spectral region beyond ~2500 cm^{-1} shows the second-order carbon bands.